DE LA RECHERCHE À L'INDUSTRIE

www.cea.fr

Numerical simulations of the rf-driven toroidal current in tokamaks

Y. Peysson, J. Decker

CEA, IRFM, F-13108, Saint-Paul-lez-Durance, France

Contact: yves.peysson@cea.fr

Outline

- **The current drive problem in tokamaks**
- **The equations for calculating a rf current source**
- **C3PO/LUKE, a rf current source module for integrated modeling**
- **Numerical simulations for the LH and EC waves** (ITER, Tore Supra, JET, TCV)
- **Advanced studies**
  - *Influence of plasma fluctuations on rf current source* (TCV, ITER)
  - *Integrated modeling for designing stable MHD scenarios* (ITER)
  - *Towards neoclassical current drive simulations*
- **Conclusion and prospects**

The current drive problem in tokamaks

The plasma current: a key parameter for tokamak operation

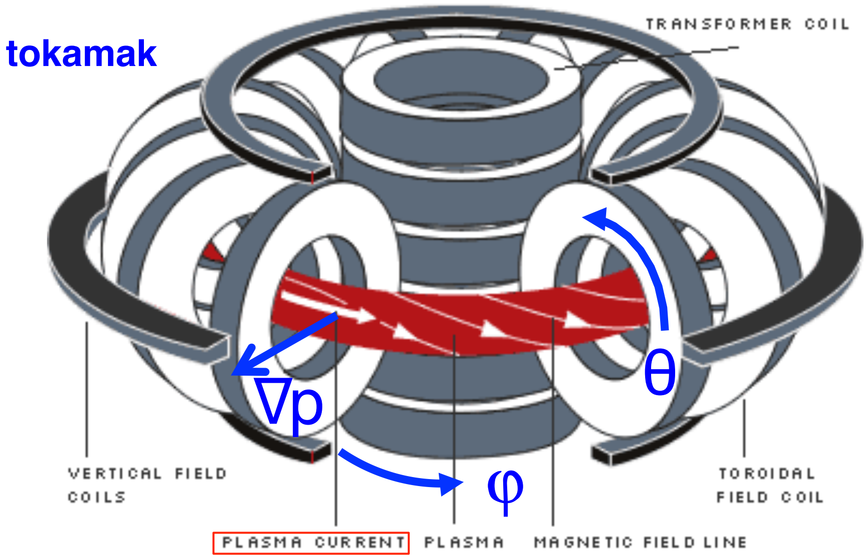

Toroidal MHD equilibrium

$$\boxed{j_{plasma}} \times B = \nabla p$$

Energy confinement

$$\tau_E \propto \boxed{I_{plasma}} / \sqrt{\boxed{P_{ext.}}}$$

Key role for stability and performances → *winding of the magnetic field lines*

$$d\varphi / d\theta \propto \int \boxed{j_{plasma}} dS$$

Control by an external source of current: $\eta = \boxed{j_{ext.}} / \boxed{P_{ext.}}$

CD efficiency

Continuous operation

Steady-state operation → the self-organized tokamak

$$j_{plasma} = \boxed{j_{configuration}} + \boxed{j_{ext.}}$$

$$\propto \nabla p$$

Self-generated (bootstrap) $\nabla \cdot j_{\perp} \neq 0 \rightarrow j_{||} \neq 0$

forced

The current drive efficiency is too lowfor achieving $j_{plasma} \approx j_{ext.}$ **with** $P_{ext.} << P_{fusion}$

P. -H. Rebut et al., Plasma Phys. Control. Fusion, 35 (1993) A3-A14

J. Decker, Y. Peysson, et al., Nucl. Fusion, 51 (2011) 073025

$P_{Lower\ Hybrid}$ = 20 MW → I_{LH} = 0.6-1.0 MA (ITER)

Self-organized (advanced tokamak) scenarios

Steep *pressure gradient ∇p*
+
low plasma current I_p

$I_{self\text{-}generated}/I_p \geq 60\%$ (Iter)

$$\tau_E \propto \boxed{H} \times I_p/\sqrt{P_{ext.}}$$

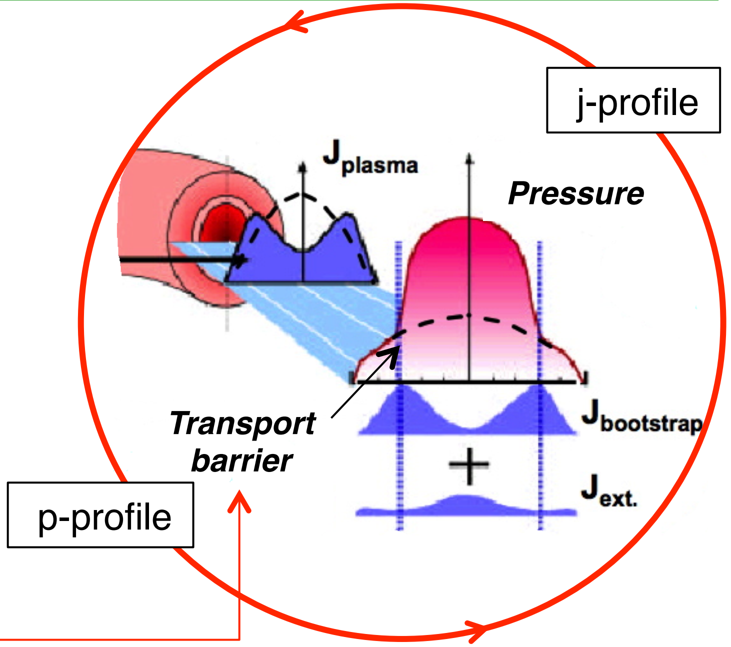

The self-organized steady-state tokamak and rf-current drive simulations

- Self-organized steady-state tokamak operation requires **integrated tokamak modeling** (j↔p)

- It put **high constraints** on the level of accuracy that should be reached by simulations of rf current drive:
  - *interpretation* of the observed phenomenology
  - reliable *prediction* capability

- **physics**: unified multi-wave description (+synergy), consistent momentum/configuration space dynamics, neoclassical corrections (high ∇p regimes), local non-axisymmetric magnetic configuration,…

- **numerics**: modular, fast and robust tools with advanced algorithms, using latest hardware progresses

From pulsed to steady-state operation beyond the transformer

0-D

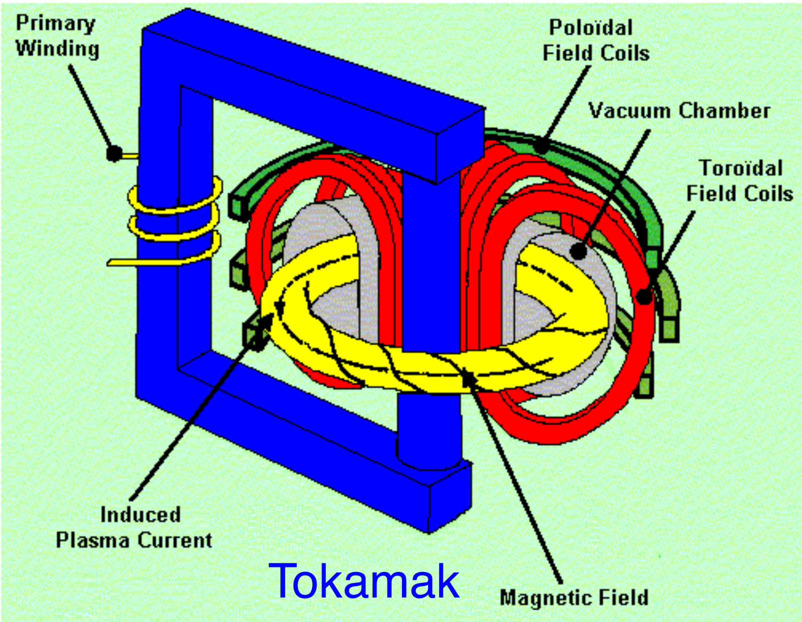

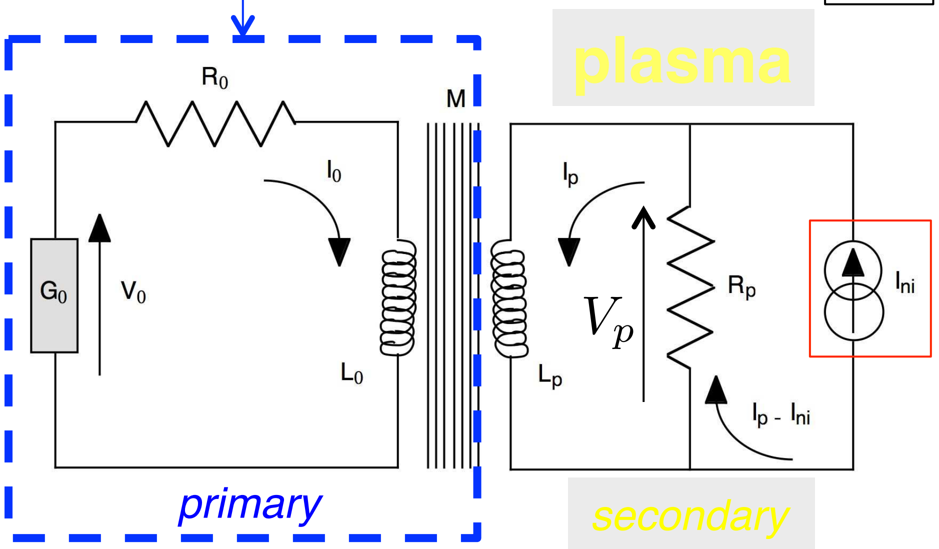

The plasma duration is limited by the consumption of the magnetic flux Φ_M

$$M\frac{dI_p}{dt} + L_0\frac{dI_0}{dt} + R_0 I_0 = V_0$$

$$M\frac{dI_0}{dt} + L_p\frac{dI_p}{dt} + \underbrace{R_p\left(I_p - I_{ni}\right)}_{V_p} = 0$$

Heating $\sim T_e^{-3/2}$

Inductive current

$$\frac{d\Phi_M}{dt} = L_0\frac{dI_0}{dt} = -\boxed{R_p}\frac{L_0}{M}\overbrace{\left(I_p - \boxed{I_{ni}}\right)}$$

Non-inductive source of current

*F. Kazarian et al., Plasma Phys. Control. Fusion **38** (1996) 2113–2131*

Convergence towards stationnary regime with a non-inductive source of current

Constant I_p feedback control

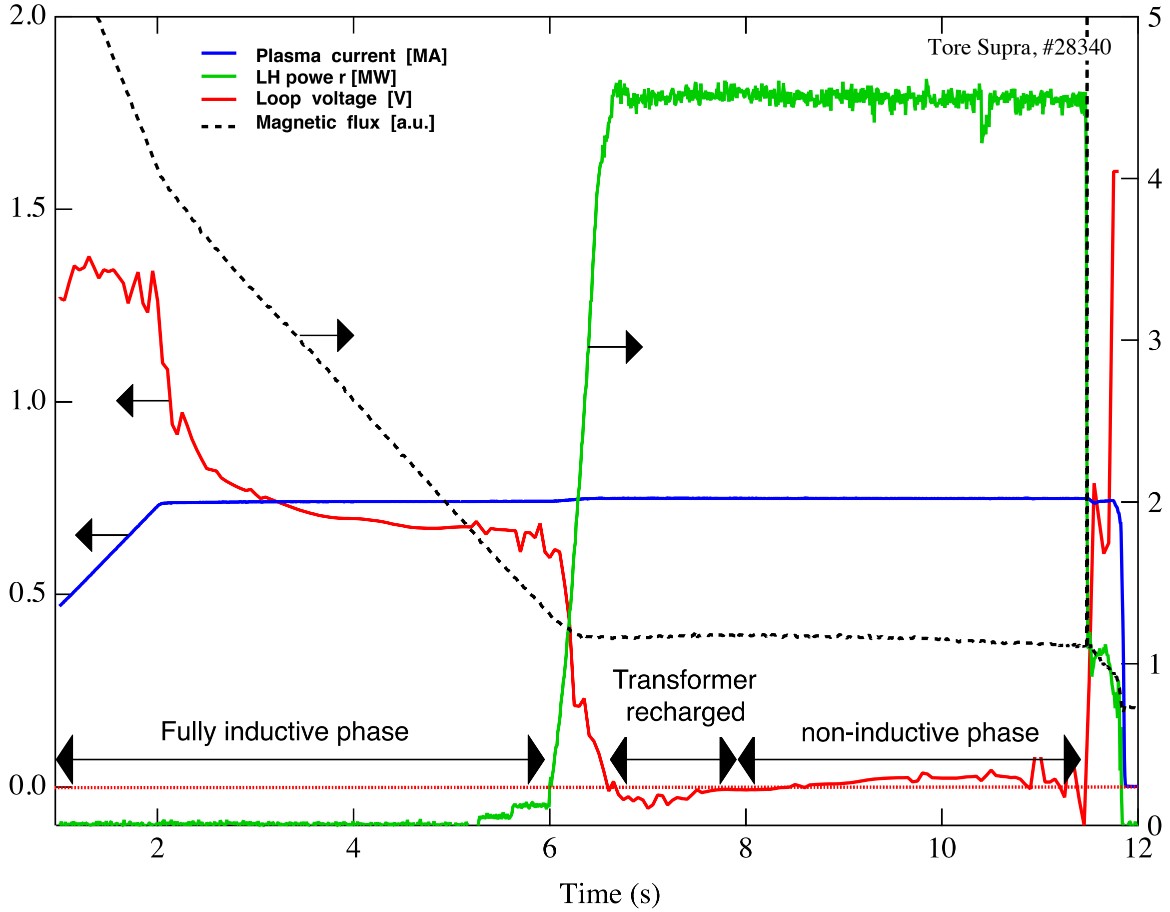

Difficult to achieve a reproducible stationnary regime

Convergence towards stationnary regime with a non-inductive source of current

Constant V_0 feedback control

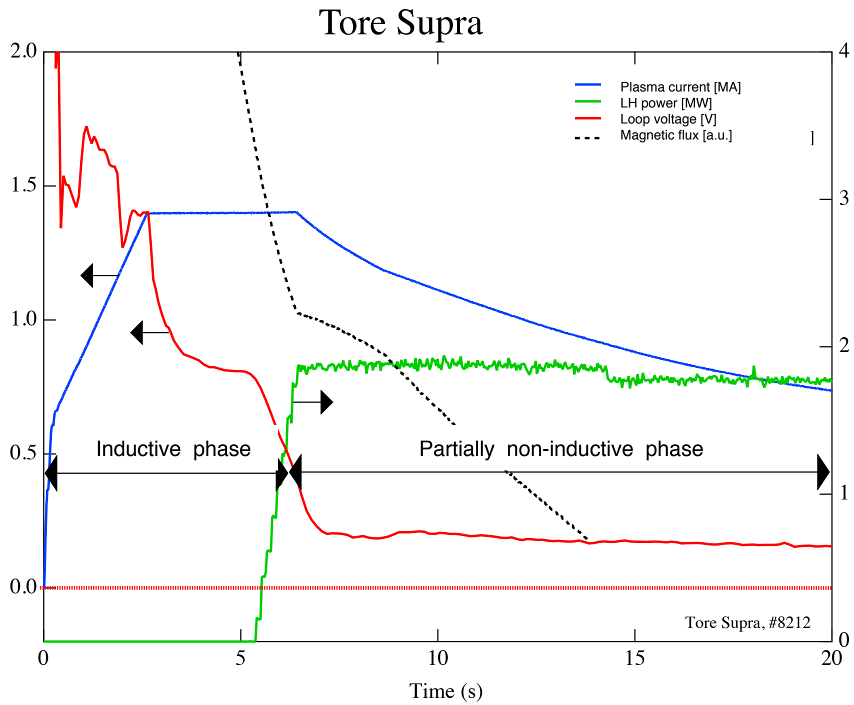

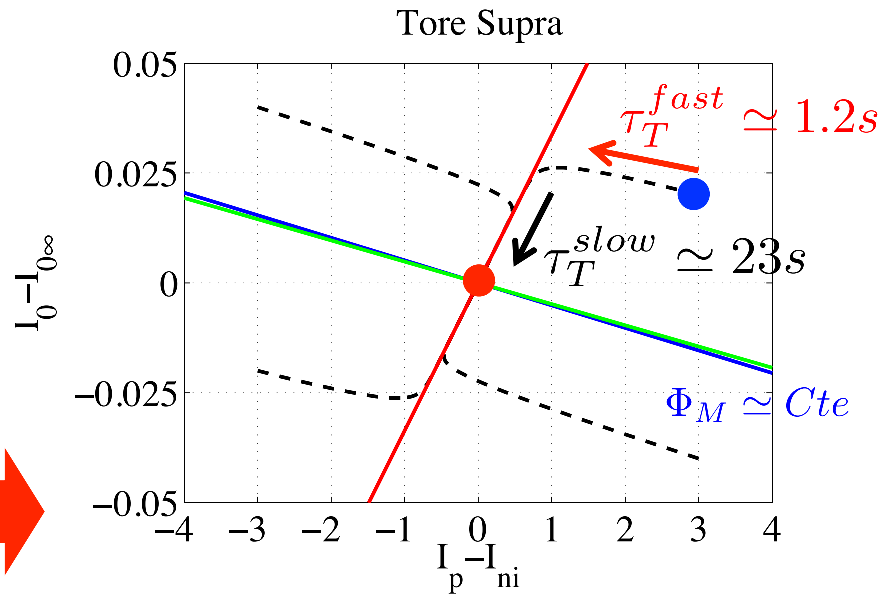

Full consumption of the magnetic flux Φ_M before reaching the stationnary regime

Two time scales associated to the transformer eigenmodes

The fast time scale corresponds to constant magnetic flux Φ_M

F. Kazarian et al., *Plasma Phys. Control. Fusion* **38** (1996) 2113–2131

Convergence towards stationnary regime with a non-inductive source of current

Constant Φ_M feedback control → single time scale $\tau_T^{fast} \simeq 1.3s$

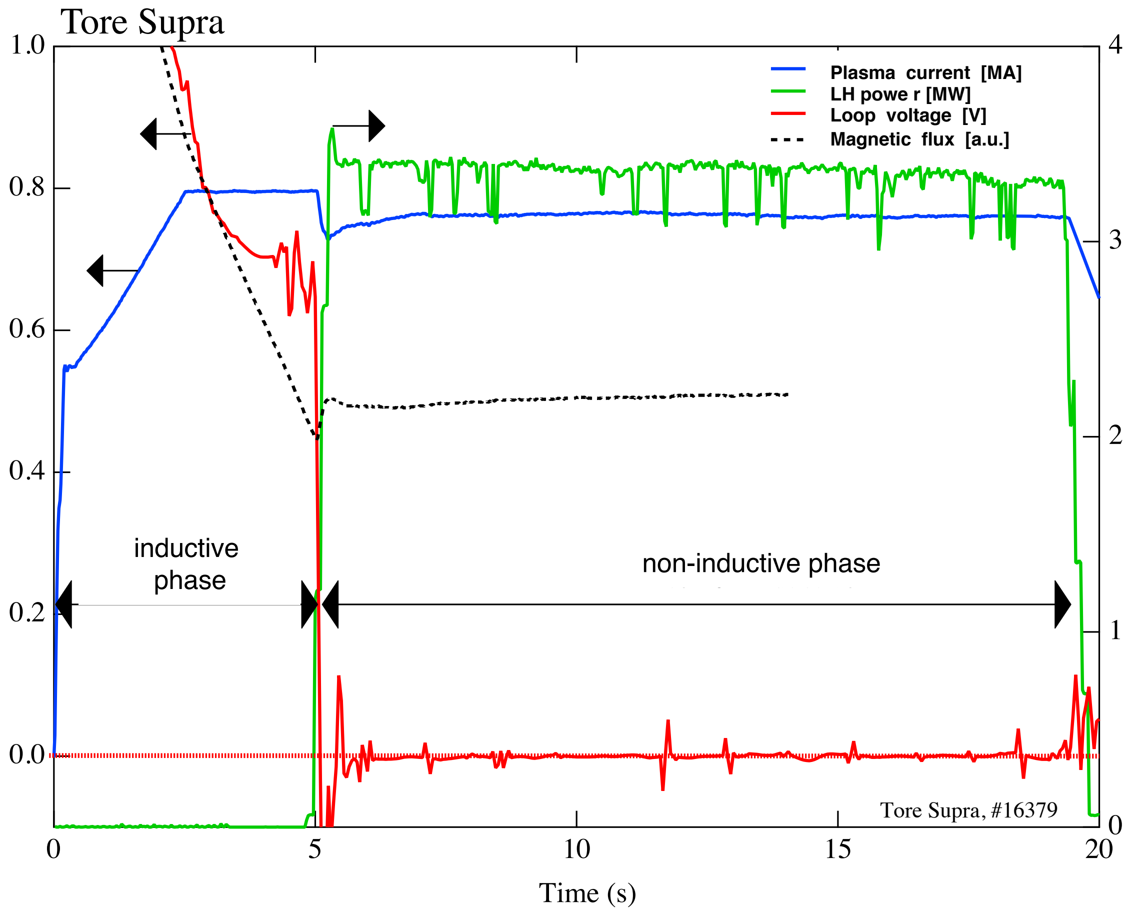

$V_p = 0V$

Reproducible stationnary regime, I_p level adjusted with $P_{LH} \rightarrow \eta$

From a stationnary to a steady-state regime: current resistive diffusion

1-D

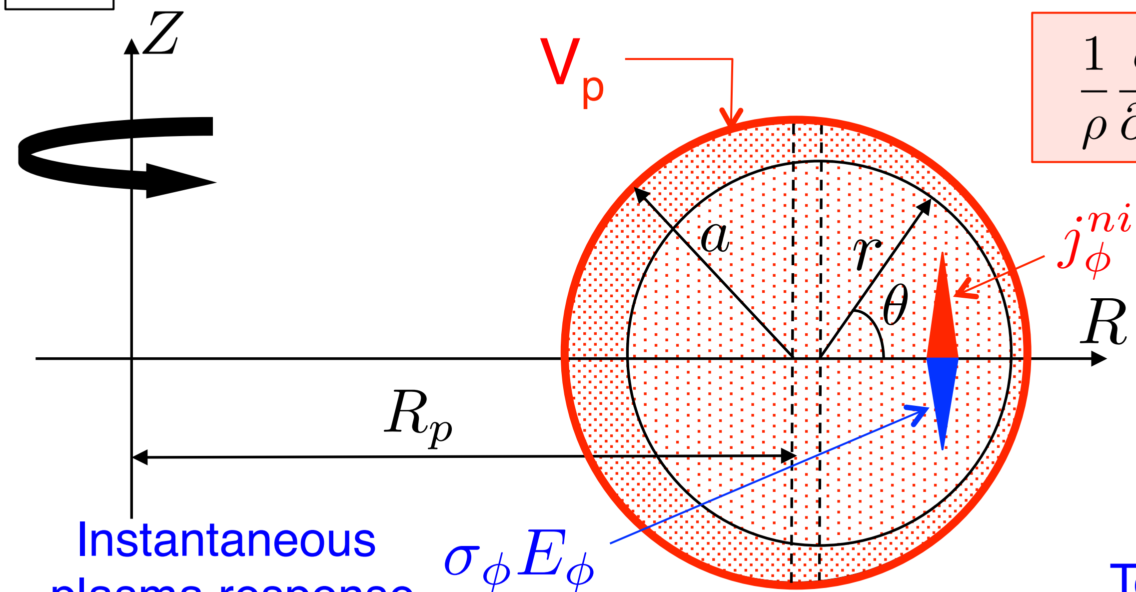

Ampère's + Faraday's + Ohm's law

$$\boxed{\frac{1}{\rho}\frac{\partial}{\partial \rho}\left(\rho \frac{\partial E_\phi}{\partial \rho}\right) = \frac{\partial}{\partial \tau}\underbrace{\left(E_\phi + j_\phi^{ni}/\sigma_\phi\right)}_{j_\phi}}$$

Resistive time: $\tau_r = \mu_0 \sigma_\phi a^2$

Fundamental eigenmode:

$$\tau_r^* = \tau_r/\lambda_1^2 \qquad J_1(\lambda_1) = 0$$

Tore Supra (a = 0.7m) @ T_e = 5 keV

$$\boxed{\tau_r \simeq 16.8s}$$

The current density profile evolves on a very long time scale at high temperature → **current profile preshaping when the plasma is cold**

Stationnary regime: $dI_p/dt = 0$

Steady-state regime: $dj_\phi/dt = 0 \longrightarrow E_\phi = 0$ everywhere

Convergence towards steady-state regime with a non-inductive source of current

Steady-state operation: $t \gg \tau_r^* \gg \tau_{fast}$

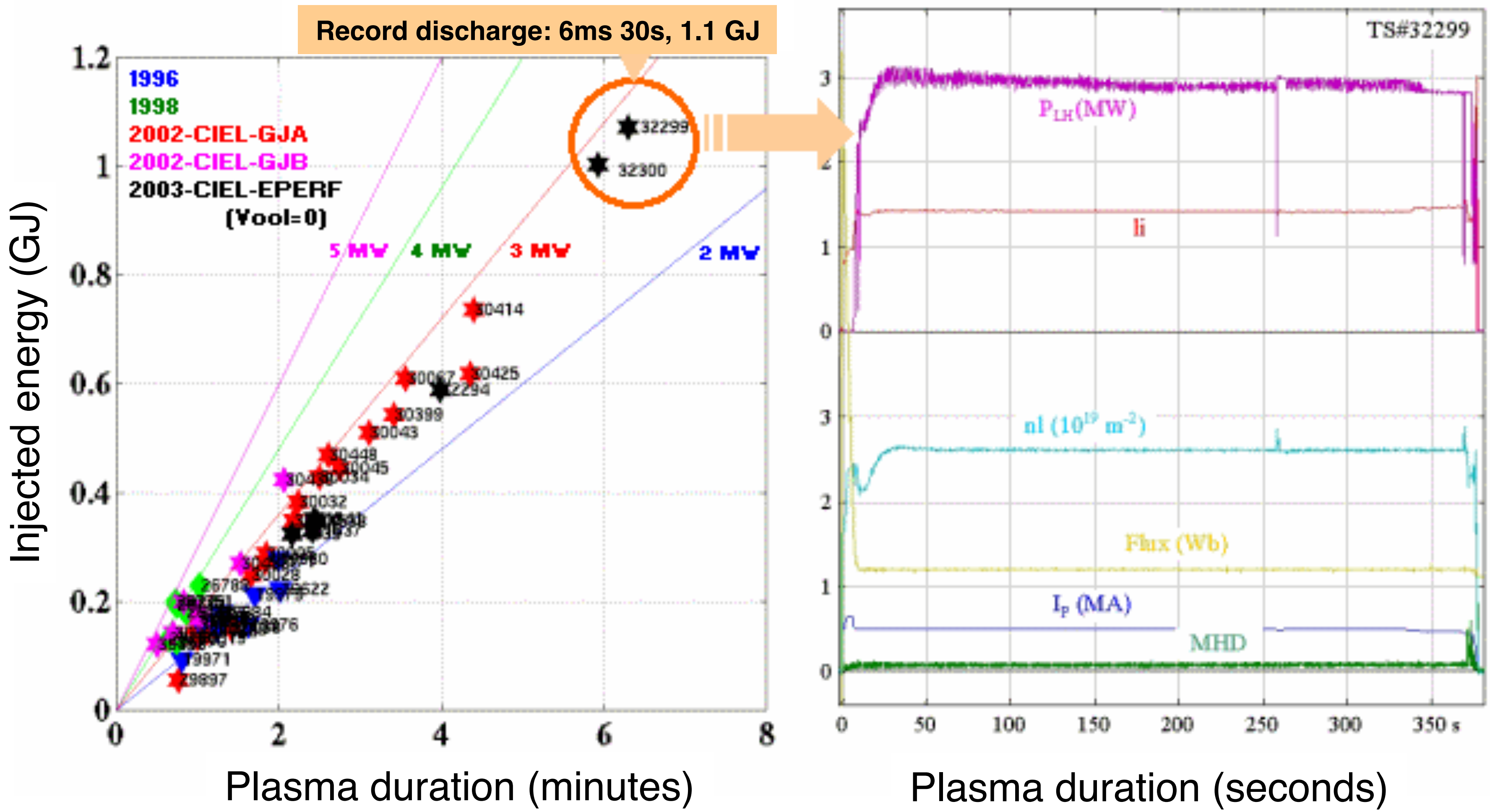

D. van Houtte et al., Fusion Engineering and Design 74 (2005) 651–658

Time scales and the physics of current sources

Millisecond — ***Second*** — ***Minute*** — ***Hour***

MHD | Transport | Current diffusion | Plasma/wall equilibrium | Erosion

TFR | *JET* | *TORE SUPRA* | *ITER*

Physics of non-inductive rf current sources

confinement

transformer

Current diffusion

$$\omega_{pe}^{-1} \leq \omega_{ce}^{-1} \ll \omega_{pi}^{-1} \leq \omega_{ci}^{-1} \ll \tau_{b,t} \ll \left(\tau_{QL}, \tau_{coll}, \tau_{E_{\parallel}}\right) \leq \tau_{art} \leq \tau_{Energy} \ll \tau_{T}^{fast} \ll \tau_{r}^{*}$$

Large time scale separability makes modeling easier !

(hot plasma in large machines)

code modularity

Y. Peysson and J. Decker, Theory of fusion plasmas, 2008, 1069, AIP, 176-187

Integrated tokamak modeling and current sources (CRONOS, ITM,…)

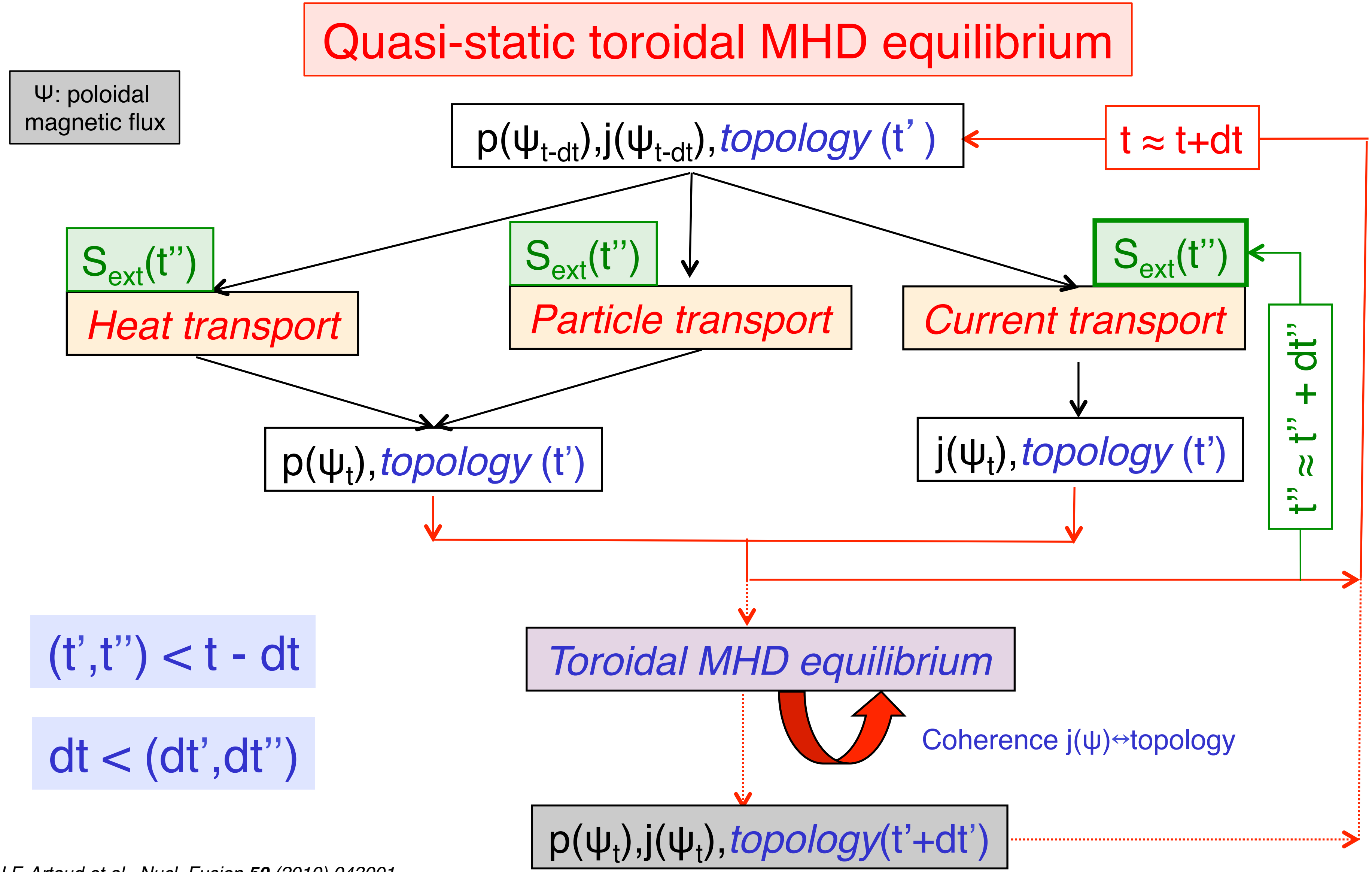

J.F. Artaud et al., Nucl. Fusion ***50*** *(2010) 043001*

Keywords to characterize an appropriate method for driving a current in tokamaks

- **Steady-state** → *for continuous operation*
- **Localization** → *capability to drive a current from the core to the edge of the plasma with broad or narrow profiles.*
- **Controlability** → *for real-time modification of the current level and spatial localization from parameters at launch*
- **Efficiency** → *the smallest possible fraction of fusion power is used for driving a current in the plasma*

rf waves provide a set of very powerful tools for current drive

Non-inductive current sources

Current drive efficiency

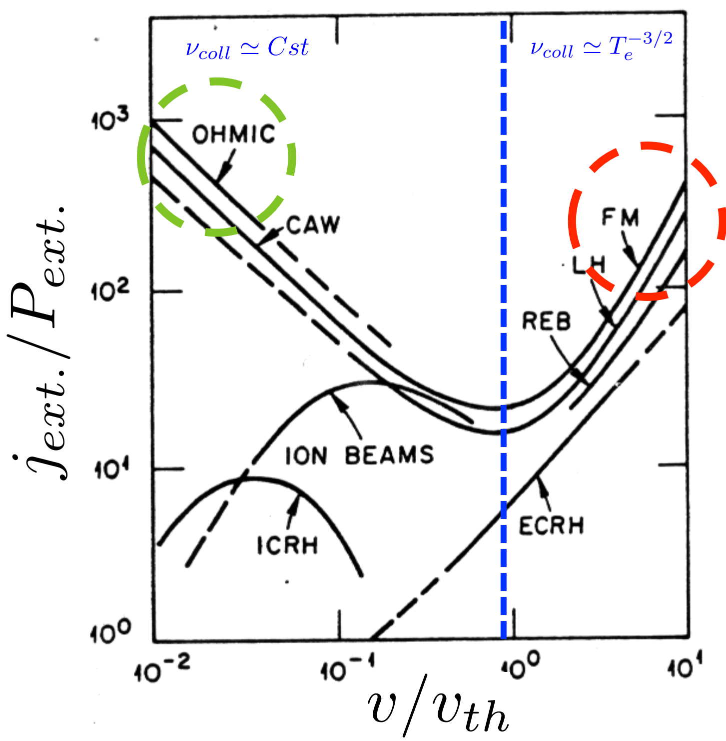

$$\Delta j_{ext.} = n\, e\, \boxed{\Delta v}$$

Fast electrons (20 → 200 keV)
(weakly collisional, $v \gg v_{th}$)

Continuous operation

Resonant acceleration by the oscillating electric field of a propagating rf wave

$\Delta v \parallel B$ ***: Landau kinetic resonance, ~ 1-10 GHz (LH), ~ 100 GHz (EBW)***

$\Delta v \perp B$ ***: Cyclotronic resonance, ~ 100 GHz (EC)***

The equations for calculating a rf current source

Theory of rf current source

$\widetilde{\mathbf{E}}\left(\mathbf{x},\mathbf{p},t\right)$

Maxwell equations

Boltzmann equations

$\mathrm{f}_s\left(\mathbf{x},\mathbf{p},t\right)$

wave electric field

Distribution functions

$$\mathbf{J}\left(\mathbf{x},t\right) = |e| \sum_s Z_s \iiint d^3\mathbf{p} f_s\left(\mathbf{x},\mathbf{p},t\right)\mathbf{p}/\gamma_s$$

$$\mathbf{P}\left(\mathbf{x},t\right) = \sum_s m_s c^2 \iiint d^3\mathbf{p}\left(\gamma_s - 1\right)\partial f_s\left(\mathbf{x},\mathbf{p},t\right)/\partial t$$

- Boltzmann equation, ion dynamics ignored ($m_e/m_s << 1$)

$$\left\{\begin{aligned} &\frac{df}{dt} = \frac{\partial f}{\partial t} + \dot{\mathbf{x}} \cdot \nabla_{\mathbf{x}} f + \dot{\mathbf{p}} \cdot \nabla_{\mathbf{p}} f = \boxed{C\left(f\right)} \\ &\dot{\mathbf{p}} = e\left(\mathbf{E} + \mathbf{v} \times \mathbf{B}\right) \\ &\dot{\mathbf{x}} = \mathbf{v} = \mathbf{p}/\gamma \end{aligned}\right.$$

Coulomb force

Fokker-Planck collision operator

$$\mathcal{O}\left(1/\log\Lambda\right)$$

- Maxwell's equations

$$\left\{\begin{aligned} &\nabla \times \mathbf{E} = -\partial \mathbf{B}/\partial t \\ &\nabla \times \mathbf{B} = \mu_0 \mathbf{J} - c^{-2} \partial \mathbf{E}/\partial t \end{aligned}\right.$$

Space- and time-scale ordering

Bounce frequency

- Small parameter expansion: $\delta^2 \simeq \rho/R \simeq \boxed{\omega_b}/\Omega$
- In tokamaks, Coulomb collisions $\nu/\Omega \leq \delta^2$

$$\left\{\begin{array}{l} \partial/\partial t = \boxed{\partial/\partial t_{\omega,\Omega}} + \boxed{\delta^2 \partial/\partial t_b} \\ \nabla_{\mathbf{x}} = \boxed{\nabla_{\mathbf{x}_\rho}} + \boxed{\delta \nabla_{\mathbf{x}_T}} + \boxed{\delta^2 \nabla_{\mathbf{x}_R}} \end{array}\right.$$

Gyro-motion

Radial transport

Orbits

Small parameter expansion

- Expansion in power of δ

$$\left\{\begin{aligned} f &= f_0 + \delta f_1 + \delta^2 f_2 + \dots \\ \mathbf{B} &= \mathbf{B}_0 + \delta \mathbf{B}_1 + \delta^2 \mathbf{B}_2 + \dots \\ \mathbf{E} &= \mathbf{E}_0 + \delta \mathbf{E}_1 + \delta^2 \mathbf{E}_2 + \dots \\ \mathbf{J} &= \mathbf{J}_0 + \delta \mathbf{J}_1 + \delta^2 \mathbf{J}_2 + \dots \\ C &= \delta^2 C_2 + \dots \end{aligned}\right.$$

- Magnetic equilibrium: $\mathbf{E}_0 = 0$

Zero-order scale: magnetic equilibrium

- to order δ^0

$$\partial f_0/\cancel{\partial t_{\omega,\Omega}} + \mathbf{v}\cdot\cancel{\nabla_{\mathbf{x}_\rho}} f_0 + \boxed{\Omega\partial f_0/\partial\varphi = 0}$$

gyro-independent

Equilibrium magnetic field and current:

$$\begin{cases} \nabla_{\mathbf{x}_R}\times\mathbf{B}_0 = \mu_0\mathbf{J}_0 \\ \mathbf{J}_0(\mathbf{x},t) = e\iiint \mathbf{v} f_0(\mathbf{x},\mathbf{p},t)\, d^3\mathbf{p} \end{cases}$$

First order scale: wave dynamics

- to order δ[1]

$$\partial f_1/\partial t_{\omega,\Omega} + \mathbf{v}\cdot\nabla_{\mathbf{x}_\rho} f_1 + \Omega\partial f_1/\partial\varphi =$$

$$-e\left[\mathbf{E}_1 + \mathbf{v}\times\mathbf{B}_1\right]\cdot\nabla_{\mathbf{p}} f_0 - \mathbf{v}\cdot\nabla_{\mathbf{x}_T} f_0$$

$$\Downarrow$$

$$\mathbf{J}_1(\mathbf{x},t) = e\iiint \mathbf{v} f_1(\mathbf{x},\mathbf{p},t)\, d^3\mathbf{p}$$

$$= \boxed{\mathbb{S}}(f_0)\cdot\mathbf{E}_1$$

constitutive relation

conductivity tensor

First order scale: wave dynamics

Maxwell equation linear in $\mathbf{E}_1$:

$$\nabla_{\mathbf{x}_\rho} \times \nabla_{\mathbf{x}_\rho} \times \mathbf{E}_1 + \mu_0 \mathbb{S}\left(f_0\right) \cdot \partial \mathbf{E}_1 / \partial t_{\Omega,\omega}$$

$$+ c^{-2} \partial^2 \mathbf{E}_1 / \partial^2 t_{\Omega,\omega} = 0$$

Second order scale: guiding-center dynamics

- to order δ^2

$$\partial f_2/\partial t_{\omega,\Omega} + \mathbf{v}\cdot\nabla_{\mathbf{x}_\rho} f_2 + \Omega\partial f_2/\partial\varphi +$$

$$\boxed{\partial f_0/\partial t_b} + \mathbf{v}\cdot\nabla_{\mathbf{x}_R} f_0 + \mathbf{v}\cdot\nabla_{\mathbf{x}_T} f_1 +$$

$$e\left[\mathbf{E}_2 + \mathbf{v}\times\mathbf{B}_2\right]\cdot\nabla_{\mathbf{p}} f_0 +$$

$$e\left[\mathbf{E}_1 + \mathbf{v}\times\mathbf{B}_1\right]\cdot\nabla_{\mathbf{p}} f_1 = C\left(f_0\right)$$

Using linear relation between f_0 and f_1 (order δ^1) + averaging over fast time scales → slow time scale evolution of f_0.

Quasilinear kinetic equation

$$\boxed{\begin{aligned}\partial f_0/\partial t_b + \mathbf{v}_{cg}\cdot\nabla_{\mathbf{x}_R} f_0 \\ = C\left(f_0\right) + Q\left(f_0\right) + T\left(f_0\right) + E\left(f_0\right)\end{aligned}}$$

$$\left\{\begin{aligned} E\left(f_0\right) &= -\nabla_{\mathbf{p}}\left(e\left\langle\mathbf{E}_2\right\rangle_{\Omega,\omega}\cdot f_0\right) \\ Q\left(f_0\right) &\equiv \nabla_{\mathbf{p}}\cdot\left(\mathbb{D}_{ql}\cdot\nabla_{\mathbf{p}} f_0\right) \longrightarrow \boxed{\mathbb{D}_{ql} \propto \left|\left|\mathbf{E}_1\right|\right|^2} \\ T\left(f_0\right) &\equiv \nabla_{\mathbf{x}_T}\cdot\left(\mathbb{D}_{\mathbf{x}}\cdot\nabla_{\mathbf{x}_T} f_0\right)\end{aligned}\right.$$

Linearization of the electron-electron collision operator

$$\mathcal{C}(f) = \sum_s \sum_{s'} C(f, f_{ss'}) + C(f, f)$$

$$C(f, f) \simeq C(f, f_M) + C(f_M, f)$$ for the electrons

$$\boxed{f \simeq f_M + \delta f}$$

$$C(f_M, f_M) = 0$$

First term of the Legendre polynomials expansion of the electron distribution function

$$\boxed{C(f_M, f) \simeq C\left(f_M, \frac{3}{2}\xi \boxed{f^{(m=1)}} (t, \mathbf{X}, p)\right)}$$

By construction the linearized electron-electron collision operator *conserves particles, momentum, but not energy*, so there is no need to **introduce an energy loss term** in the Fokker-Planck equation.

C.F.F. Karney, Comp. Phys. Rep., 1986, 4, pp. 183-244

Range of validity

- quasilinear approximation valid for small wave field amplitude
- no electron trapping in the rf wave field (collisions)
- Guiding center approximation

(order δ²)

$$\mathbf{v}_{cg} \simeq p_{\|}\hat{\mathbf{b}}/\gamma + \boxed{\mathbf{v}_D}$$

Further expansion for bootstrap current

$$\mathbf{p} = p_{\|}\hat{\mathbf{b}} + \mathbf{p}_{\perp}$$

- pitch-angle cosine: $\xi = p_{\|}/p$

$f_0\left(\psi, \theta, \phi, p_{\|}, p_{\perp}\right)$ is function of five coordinates

Further reduction of the number of dimensions: bounce-averaging

- axisymmetric configuration $\longrightarrow$ averaging over ϕ
- New ordering: low collision or « banana » regime

$$\delta^2 \ll \nu^* = \nu\tau_b \ll 1$$

- Thin banana width approximation $\|\mathbf{v}_D\| / \|\mathbf{v}_{cg}\| \ll 1$

$$\left\{\begin{array}{l}
\partial\{f_0\}/\partial t = \{C(f_0)\} + \{Q(f_0)\} + \{E(f_0)\} \\
\{\mathbf{v}_{cg}\cdot\nabla_{\mathbf{x}_R} f_0\} = 0 \\
\{\mathcal{O}\} \equiv \dfrac{1}{\lambda\tilde{q}} \underbrace{\left[\dfrac{1}{2}\sum\nolimits_\sigma\right]_T}_{\text{trapped electrons}} \displaystyle\int_{\theta_{\min}}^{\theta_{\max}} \dfrac{d\theta}{2\pi} \dfrac{1}{\left|\hat{\psi}\cdot\hat{\mathbf{r}}\right|} \dfrac{r}{a_p} \dfrac{B}{B_P} \dfrac{\xi_0}{\xi} \mathcal{O}
\end{array}\right.$$

J. Decker, and Y. Peysson, report EUR-CEA-FC-1736, Euratom-CEA (2004)

Electron orbits

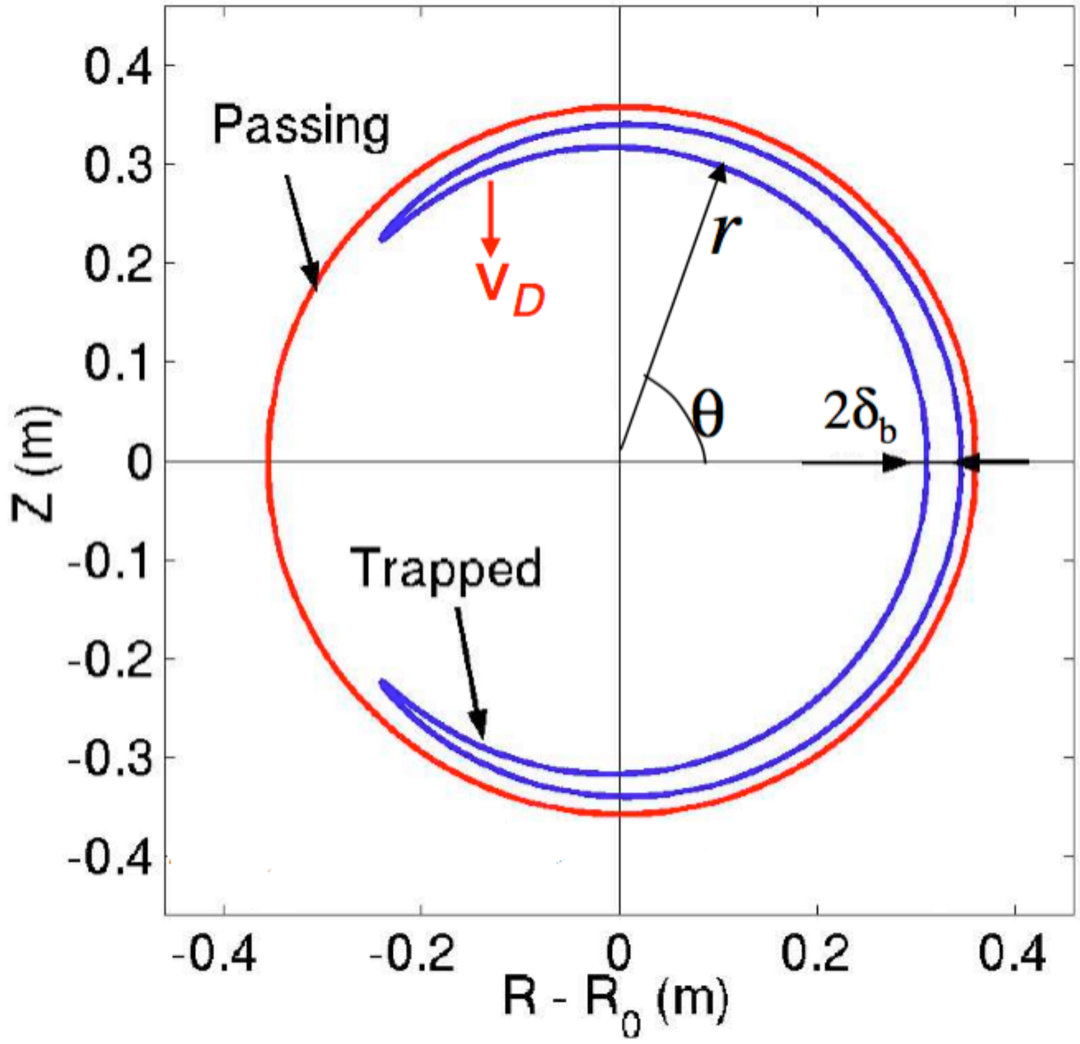

Reduced configuration space: 3-D

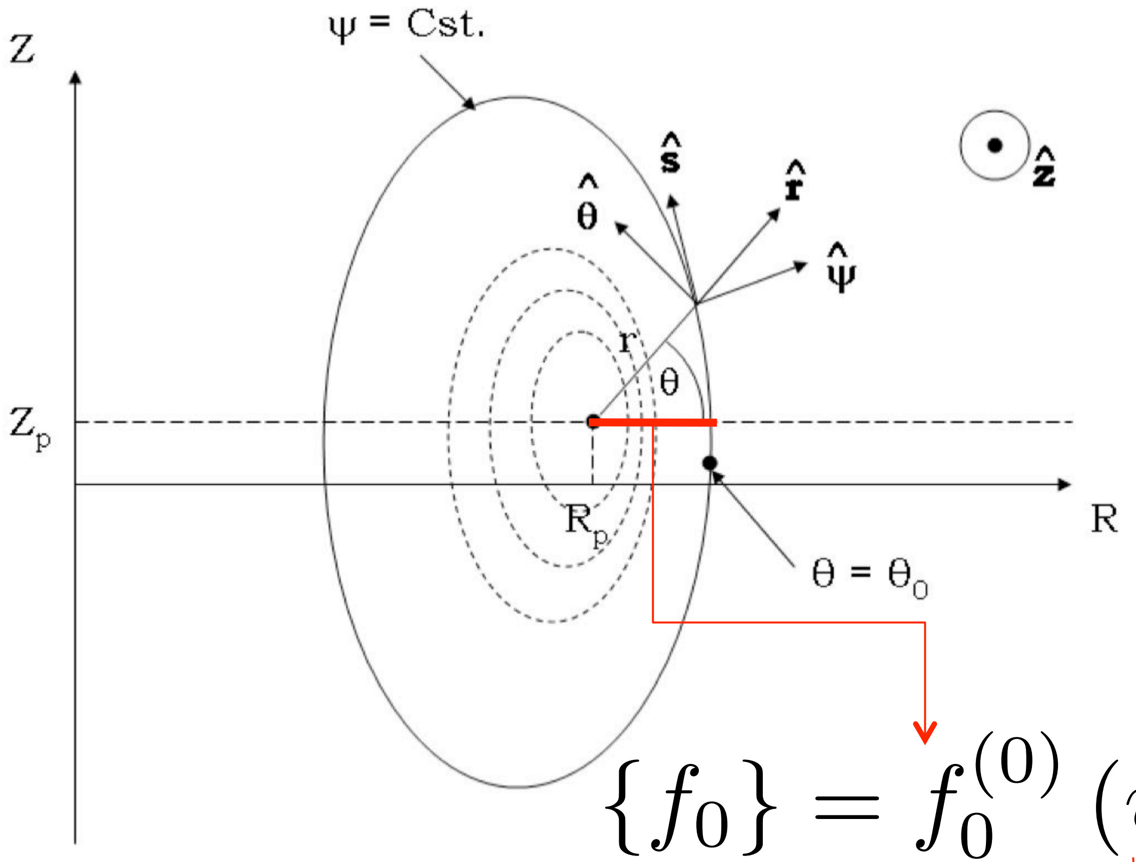

$$\{f_0\} = f_0^{(0)}\underbrace{(\psi, p, \xi_0)}_{\textit{3-D}}$$

All the electron dynamics is projected at $B = B_{min}$

Bounce-averaged electron momentum distribution function

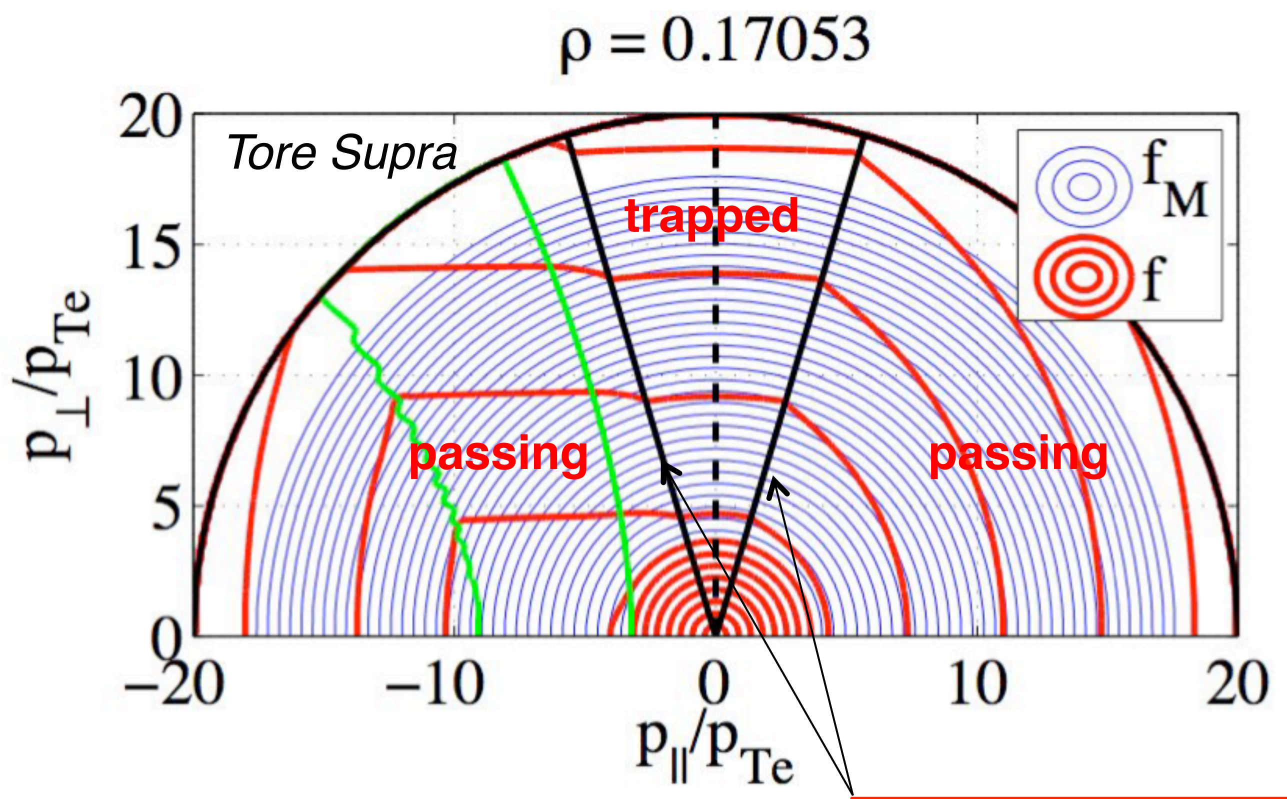

$$\xi_{0T} = \sqrt{1 - \frac{B_{\min}(\psi)}{B_{\max}(\psi)}}$$

Momentum space dynamics on the magnetic flux surface ψ

Local reconstruction of the electron distribution at any poloidal position

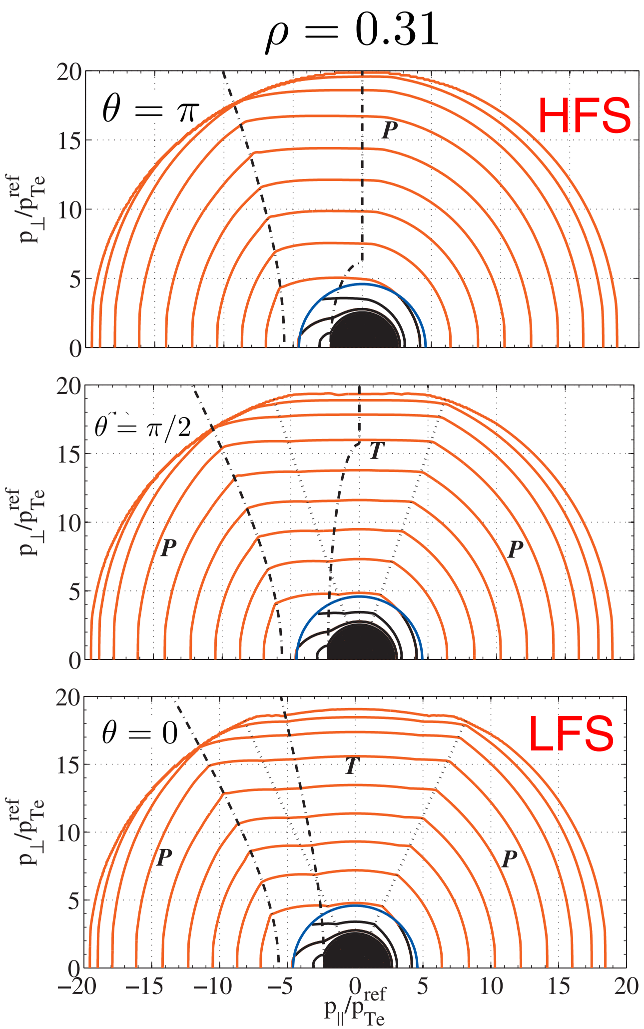

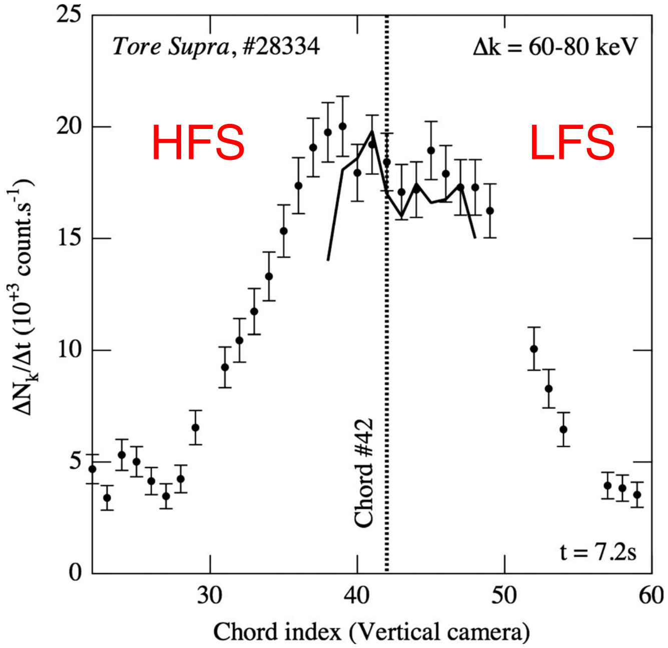

$$f(\psi,\theta,p,\xi) = f^{(0)}(\psi,p,\xi_0)$$

$$\xi = \sigma\sqrt{1-\Psi(\psi,\theta)(1-\xi_0^2)}$$

LUKE *3-D Fokker-Planck solver*
R5-X2 *bremsstrahlung code*

Y. Peysson and J. Decker, Phys. Plasma, ***15****, 092509 (2008)*

Bounce-averaging range of validity

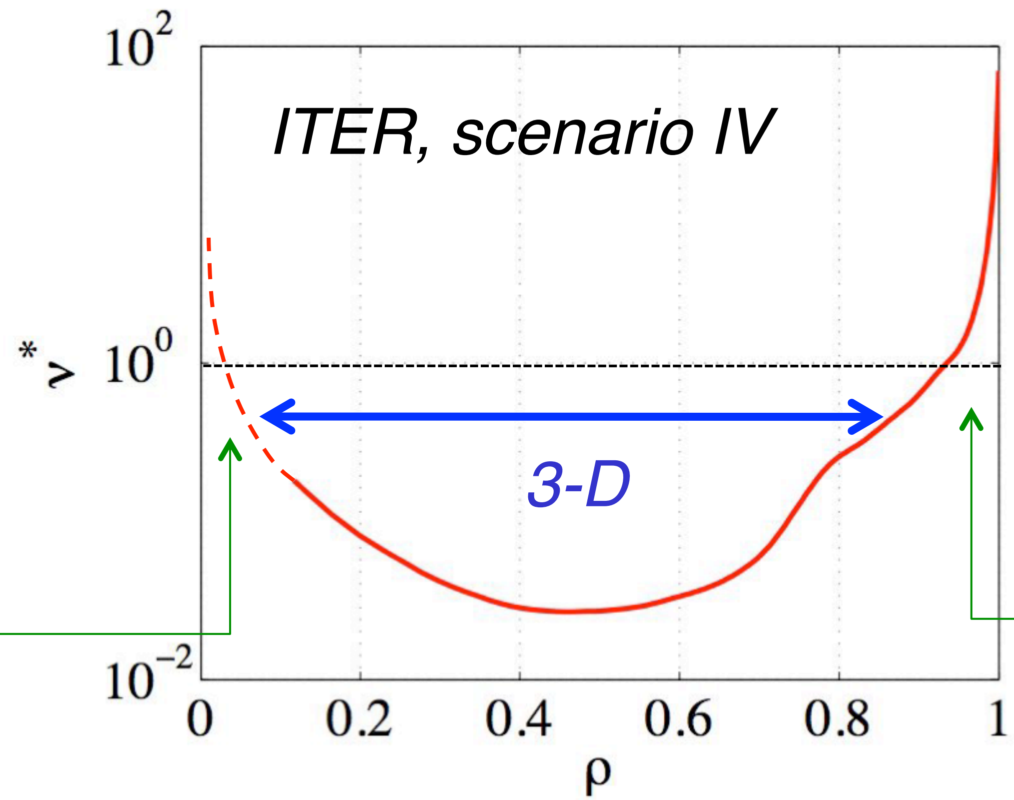

Fast detrapping (collision, turbulence,…)

4-D kinetic codes

Strong collision frequency (low temperature plasma)

Y. Peysson and J. Decker, Theory of fusion plasmas, 2008, 1069, AIP, 176-187

rf wave ordering and code complexity

$$(\boxed{\lambda}, \boxed{\phi_B}, \boxed{R})$$

wave length | beam width | gradients length

Increasing level of complexity

$\lambda \ll \phi_B \ll R$ ⇨ ray-tracing

$\lambda \sim \phi_B \ll R$ ⇨ beam-tracing

$\lambda \ll \phi_B \sim R$ ⇨ WKB full-wave

$\lambda \sim \phi_B \sim R$ ⇨ full-wave

Quasi-plane wave + WKB approximations: ray tracing may be applied

A wave front exists: $\nabla S = k_1$

$$\mathbf{E}_1(\mathbf{x},t) = \boxed{\mathbf{E}_{\mathbf{k},\omega}(\mathbf{x},t)}\, e^{i[\boxed{\mathbf{k}_1(\mathbf{x},t)}\cdot\mathbf{x} - \boxed{\omega(\mathbf{x},t)}t]}$$

Quasi plane wave approximation

Smooth wavefield envelope

$$\boxed{\lambda \ll \phi_B}$$

~ narrow spectral width

$$\boxed{\|\Delta\mathbf{k}_1 \times \mathbf{v}_G\| / \|\mathbf{k}_1 \times \mathbf{v}_G\| \sim \lambda/\phi_B \ll 1}$$

WKB approximation

methods for uniform plasmas can be applied locally:

- *Fourier space description*
- *group velocity*
- *local conductivity tensor*

$$\boxed{\lambda \ll R}$$

Wave equation

$$\left|\nabla_{\mathbf{x}}\mathbf{E}_{\mathbf{k},\omega}\cdot\mathbf{v}_G\right| / \left|\mathbf{E}_{\mathbf{k},\omega}\cdot\mathbf{v}_G\right| \ll \left\|\mathbf{k}_1\right\|$$

$$\left|\partial\mathbf{E}_{\mathbf{k},\omega}/\partial t\cdot\mathbf{v}_G\right| / \left|\mathbf{E}_{\mathbf{k},\omega}\cdot\mathbf{v}_G\right| \ll \omega$$

$$\Downarrow$$

Wave equation

$$\boxed{\mathbb{D}_{\mathbf{k},\omega}\cdot\mathbf{E}_{\mathbf{k},\omega} = i\nabla_{\mathbf{k}}\mathbb{D}_{\mathbf{k},\omega} : \nabla_{\mathbf{x}}\mathbf{E}_{\mathbf{k},\omega}}$$

Y. Peysson and J. Decker, Theory of fusion plasmas, 2008, 1069, AIP, 176-187

rf physics definitions

- dispersion tensor

$$\mathbb{D}_{\mathbf{k},\omega} = \mathbf{nn} - n^2\mathbb{I} + \mathbb{K}_{\mathbf{k},\omega}\left(f_0\right)$$

- Permitivity and susceptibility tensors

$$\mathbb{K}_{\mathbf{k},\omega}\left(f_0\right) = \mathbb{I} + \mathbb{X}_{\mathbf{k},\omega}\left(f_0\right)$$

$$\mathbb{X}_{\mathbf{k},\omega}\left(f_0\right) = i\mathbb{S}_{\mathbf{k},\omega}\left(f_0\right) / \left(\varepsilon_0\omega\right)$$

- wave refractive index

$$\mathbf{n} = \frac{c}{\omega}\mathbf{k}_1 n_{\|}\hat{\mathbf{b}} + \mathbf{n}_{\perp}$$

- wave polarization vector

$$\mathbf{e}_{\mathbf{k},\omega} = \mathbf{E}_{\mathbf{k},\omega} / \left\|\mathbf{E}_{\mathbf{k},\omega}\right\|$$

Weak damping ordering

- Assume ω and $n_{||}$ are real (rf wave propagates)
- weak damping approximation:

$$\delta \sim \left| \mathbb{D}^A_{\mathbf{k},\omega}(i,j) \right| / \left| \mathbb{D}^H_{\mathbf{k},\omega}(i,j) \right| \ll 1$$

where $\mathbb{D}_{\mathbf{k},\omega} = \mathbb{D}^H_{\mathbf{k},\omega} + i\mathbb{D}^A_{\mathbf{k},\omega}$

Expansion in powers of δ $\longrightarrow \left\{ \begin{array}{l} n_\perp = n_{\perp r} + i n_{\perp i} \\ \mathbf{e}_{\mathbf{k},\omega} \\ \mathbb{D}_{\mathbf{k},\omega} \end{array} \right.$

*Decker, J. and Ram, A., Phys. Plasmas, **2006**, 13, 112503*

Ray tracing equations

- to order δ^0

$$\mathbb{D}^{H}_{\mathbf{k},\omega}\left(n_{\perp 0}\right)\cdot\mathbf{e}_{\mathbf{k},\omega,0}=0$$

dispersion relation satisfied by propagative eigenmodes

$$\det\left(\mathbb{D}^{H}_{\mathbf{k},\omega}\right)=\mathcal{D}(n_{\perp 0},n_{\parallel},\omega)=0$$

$$n_{\perp 0}=n_{\perp 0}\left(n_{\parallel},\omega\right)$$

$$n_{\perp i0}=0$$ no rf absorption at this order !

Wave-particle interaction

- to order δ^1

Equation of energy transfer between wave and electrons

$$\mathbf{v}_G \cdot \nabla_{\mathbf{x}} \left\| \mathbf{E}_1 \right\| + \frac{\mathbf{e}^*_{\mathbf{k},\omega,0} \cdot \mathbb{D}^A_{\mathbf{k},\omega} \cdot \mathbf{e}_{\mathbf{k},\omega,0}}{\partial \left(\mathbf{e}^*_{\mathbf{k},\omega,0} \cdot \mathbb{D}^H_{\mathbf{k},\omega} \cdot \mathbf{e}_{\mathbf{k},\omega,0} \right) / \partial \omega} \left\| \mathbf{E}_1 \right\| = 0$$

Weak damping approximation

Separation propagation/absorption

Y. Peysson and J. Decker, Theory of fusion plasmas, 2008, 1069, AIP, 176-187

Resonance condition: quasilinear self-consistency

- non-resonant contribution

$$\mathbb{D}^{H}_{\mathbf{k},\omega} \longrightarrow \text{principal value of } \mathbb{S}_{\mathbf{k},\omega}$$

$$\boxed{\mathbb{D}^{H}_{\mathbf{k},\omega}\left(f_0\right) \simeq \mathbb{D}^{H}_{\mathbf{k},\omega}\left(f_M\right)}$$

- resonant contribution $\gamma - n_{||}p_{||} - n\Omega/\omega = 0$

$$\mathbb{D}^{A}_{\mathbf{k},\omega} \longrightarrow \text{resonant part of } \mathbb{S}_{\mathbf{k},\omega}$$

$$\boxed{\mathbb{D}^{A}_{\mathbf{k},\omega}\left(f_0\right) \neq \mathbb{D}^{A}_{\mathbf{k},\omega}\left(f_M\right)}$$ self-consistency needed !

*Decker, J. and Ram, A., Phys. Plasmas, **2006**, 13, 112503*

C3PO/LUKE,
a rf current source module
for integrated modeling

rf current source module

- the ray-tracing is function of f_M.
- the wave amplitude, i.e. the quasilinear diffusion coefficient D_{ql} must be calculated self-consistently with the distribution f_0.
- <u>Global consistency</u>: *power lost by the wave = power gained by electrons from quasilinear operator*

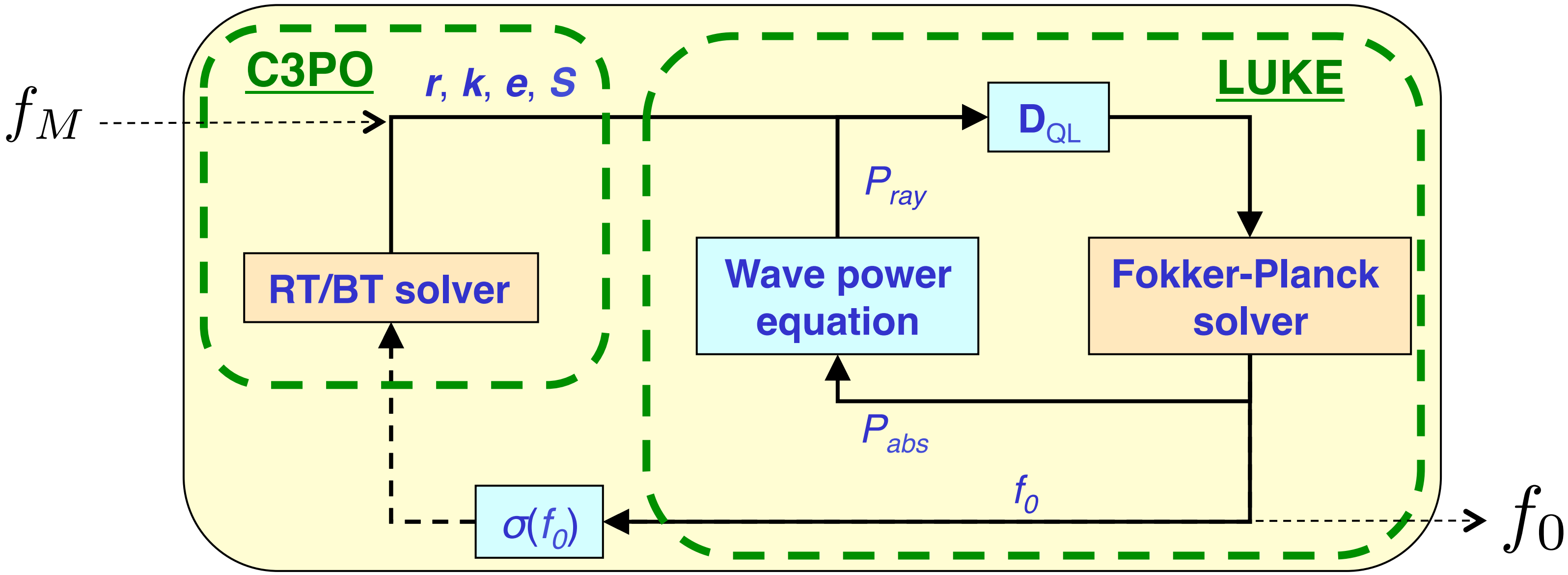

The ray tracing C3PO: multimodel approach based on chain derivatives

- Separation between plasma dispersion models and the metric associated to the magnetic equilibrium

$$\frac{\partial \mathbb{X}_{ij}^{s}}{\partial \mathbf{Y}} = \frac{\partial \mathbb{X}_{ij}^{s}}{\partial n_{\perp}}\frac{\partial n_{\perp}}{\partial \mathbf{Y}} + \frac{\partial \mathbb{X}_{ij}^{s}}{\partial n_{\parallel}}\frac{\partial n_{\parallel}}{\partial \mathbf{Y}} + \frac{\partial \mathbb{X}_{ij}^{s}}{\partial \beta_{Ts}}\frac{\partial \beta_{Ts}}{\partial \mathbf{Y}} + \frac{\partial \mathbb{X}_{ij}^{s}}{\partial \overline{\omega}_{ps}}\frac{\partial \overline{\omega}_{ps}}{\partial \mathbf{Y}} + \frac{\partial \mathbb{X}_{ij}^{s}}{\partial \overline{\Omega}_{s}}\frac{\partial \overline{\Omega}_{s}}{\partial \mathbf{Y}}$$

$$\mathbf{Y} = (\mathbf{X}, \mathbf{k}, t, \omega)$$

$$\beta_s = \sqrt{kT_s/m_s c^2}$$

$$\overline{\omega}_{ps} = \omega_{ps}/\omega \qquad \overline{\Omega}_s = \Omega_s/\omega$$

Y. Peysson et al., 2012 Plasma Phys. Control. Fusion 54 045003

The 3-D ray-tracing C3PO

- Curvilinear coordinate system: $\left(\rho\left(\psi\right),\theta,\phi\right)$
- 2-D axisymmetric configuration (cylinder, dipole, torus) + 3-D perturbation (nested magnetic flux surfaces)
- Vectorization of the magnetic equilibrium: Fourier series + piecewise cubic interpolation using Hermite polynomials: no interpolation performed at each time step
- (4,5) order Runge-Kutta
- rays are calculated inside the separatrix. Specular reflexion enforced - if needed - at ρ=1.
- ray calculation are almost stopped when the rf power is linearly damped
- cold, warm, hot and relativistic dielectric tensors
- written in C (MatLab mex-file)
- *distributed and remote computing capability* (1ray/core, GPU)

[b_1,b_2,…] = any_Matlab_function(a_1,a_2,a_3…)

Computation may be done anywhere !

{[b_1,b_2,…]} = remotecomputing(@any_Matlab_function,{a_1,a_2,a_3…},2,{a_{2_range}},computer_id)

The 3-D linearized bounce-averaged relativistic Fokker-Planck solver LUKE

- Fully 3-D conservative formulation

Magnetic ripple losses
Runaway electron avalanches

$$\partial f^{(0)}/\partial t + \nabla \cdot \mathbf{S}^{(0)} = s_+^{(0)} - \boxed{s_-^{(0)}}$$

momentum space

configuration space

$$\nabla \cdot \mathbf{S}^{(0)} = \boxed{\frac{B_0}{\tilde{q}\boxed{\lambda}} \frac{\partial}{\partial \psi} \left(\frac{\tilde{q}\boxed{\lambda}}{B_0} \|\nabla\psi\| S_\psi^{(0)} \right)}$$
$$\boxed{+ \frac{1}{p^2} \frac{\partial}{\partial p} \left(p^2 S_p^{(0)} \right) - \frac{1}{\boxed{\lambda} p} \frac{\partial}{\partial \xi_0} \left(\boxed{\lambda} \sqrt{1 - \xi_0^2} S_\xi^{(0)} \right)}$$

Orbit effect

$$\mathbf{S}^{(0)} = -\mathbb{D}^{(0)} \cdot \nabla f^{(0)} + \mathbf{F}^{(0)} f^{(0)}$$

J. Decker, and Y. Peysson, report EUR-CEA-FC-1736, Euratom-CEA (2004)

The 3-D linearized bounce-averaged relativistic Fokker-Planck solver LUKE

- **Linearized relativistic collision operator**
- **Kennel-Engelman-Lerche relativistic rf diffusion operator**
- Curvilinear coordinate system (ψ, θ, ϕ)
- 2-D axisymmetric configuration (cylinder, torus, dipole)
- 3-D perturbation (nested magnetic flux surfaces)
- Non-uniform grids (f and fluxes)
- Fully implicit time scheme: *stable for large time step Δt*
- Usual Chang & Cooper interpolation for p grid *(f_M)*
- Linear interpolation for radial and pitch-angle grids
- Discrete cross-derivatives consistent with boundary conditions *(stable scheme for D_{ql} >> 1)*
- Generalized incomplete LU factorization technique for an arbitrary number of non-zero diagonals *(highly sparse L and U matrices, low memory consumption)*
- written in MatLab
- Iterative inversion method (MatLab build-in or external solvers **MUMPS**, PETSc, SUPERLU, PARDISO)
- *Distributed, parallel and remote computing (GPU for D_{ql} operator)*

Fokker-Planck matrix to be inverted

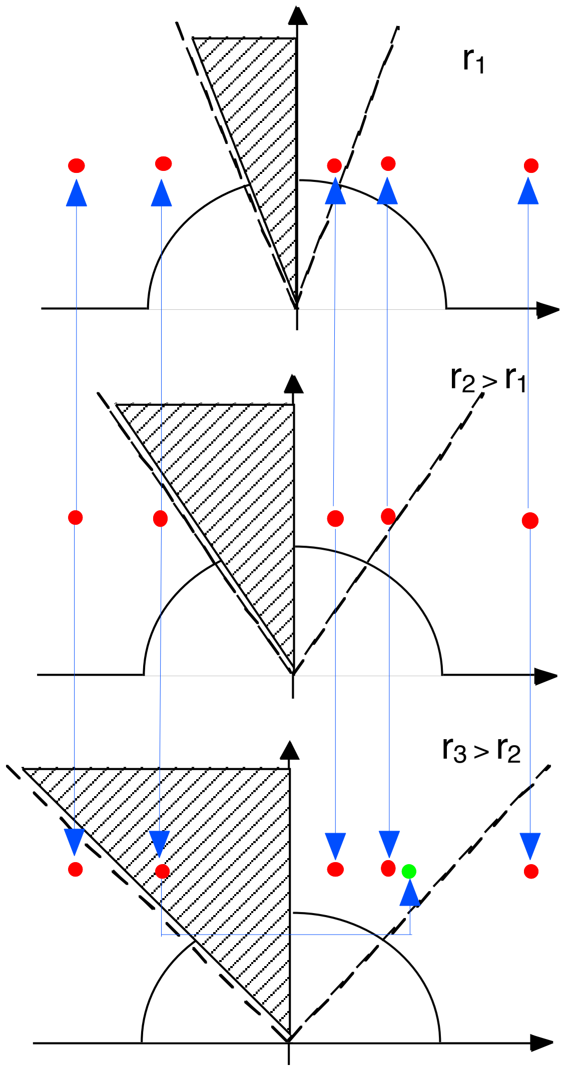

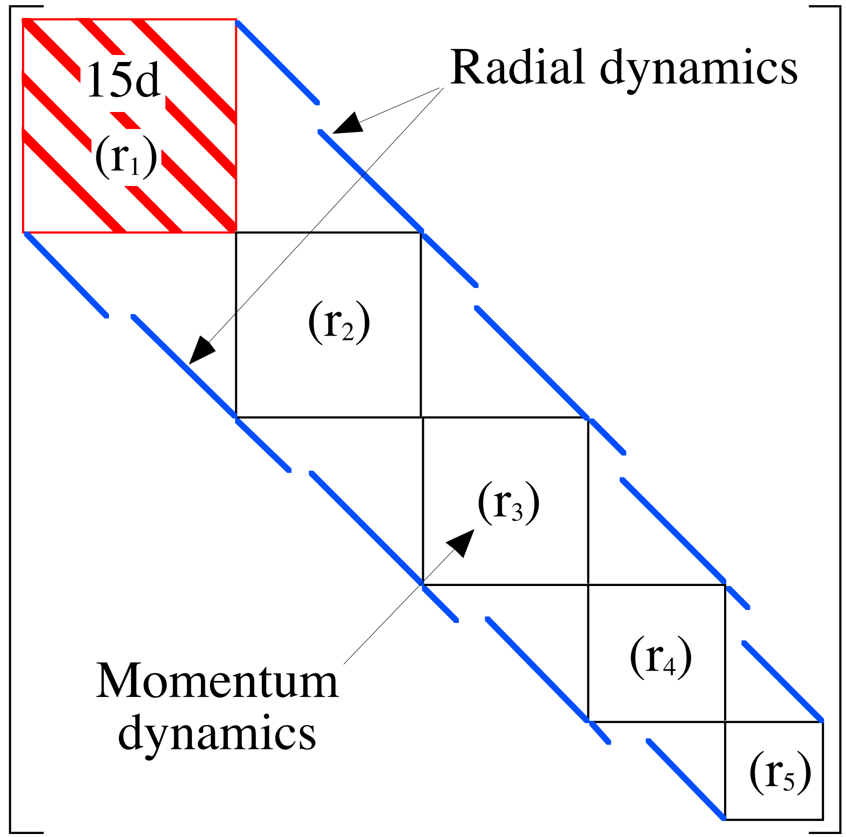

→ *up to 10^{+6}x10^{+6} entries, highly sparse matrix*

Y. Peysson, et al., 15th Top. Conf. on Radio Frequency Power in Plasmas, 2003, vol. 694 of AIP Conf. Proc., pp. 495–498.

Link between RT and FP codes

- The RF wave is described by a set of rays
- The plasma is divided into incremental flux surfaces
- D_{ql} is calculated on each flux surface (plane wave model):
    - contribution of all rays
    - contribution of all passes of the same ray

$$\mathbf{D}_{QL}(\psi,\vec{p}) = \sum_{y} \mathbf{D}_{QL}^{y}(P_y,\psi,\vec{p})$$

Ray power flow equation

$$\frac{dP_y(\psi)}{dV(\psi)} = P_y^{abs}(\psi)$$

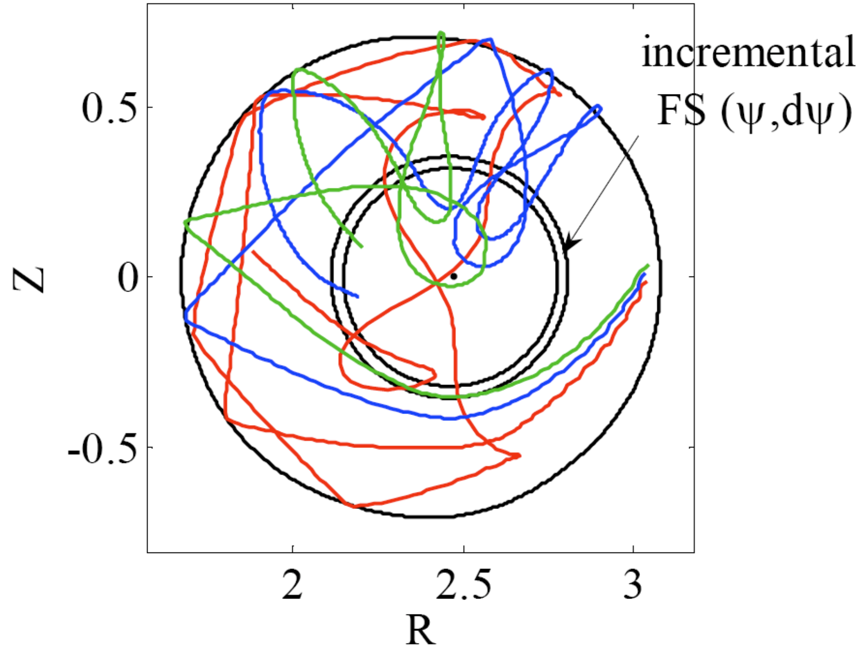

J. Decker, and Y. Peysson, in Proc. 33rd EPS Conf. on Plasma Phys. and Contr. Fusion, 2006.

Self-consistent quasilinear calculations

$$P^{abs}_{y,lin}(\psi)$$

linear absorption

ray power

$$\frac{dP_y(\psi)}{dV(\psi)} = P^{abs}_y(\psi)$$

QL diffusion coefficient

$$\mathbf{D}_{QL}(\psi,\vec{p}) = \sum_y \mathbf{D}^y_{QL}(P_y,\psi,\vec{p})$$

Fokker-Planck equation

$$C(f) + \frac{\partial}{\partial\vec{p}}\left[\mathbf{D}_{QL}\frac{\partial f}{\partial\vec{p}}\right] + T(f) = 0$$

$$J(\psi)$$

QL absorption

$$P^{abs}_y(\psi) = \int \varepsilon(p)\frac{\partial}{\partial\vec{p}}\left[\mathbf{D}^y_{QL}\frac{\partial f}{\partial\vec{p}}\right] d^3p$$

“Few ray” simulations

- **The quasilinear convergence is carried out using the power flow along each ray** (not on the global power absorption profile)

- **This technique requires the use of a reduced number of rays otherwise numerical convergence becomes weak:** LH wave → one ray per poloidal antenna row and per significant positive and negative lobes. EC antenna → beamlet for Gaussian optics in vacuum (plasma effects neglected).

⬇

- consistency with Fourier theory (spectral width overlap)
- considerable reduction of the computational effort
- **$\Delta n_{\parallel}$ is a physical spectral width ($\Delta n_{\parallel}$ dependencies)**

Numerical simulations for the LH and EC waves

(ITER, Tore Supra, JET, TCV)

Linear limit validation (LH, EC)

In the limit of low RF power level (D≈0), the result from the relativistic linear theory is well recovered

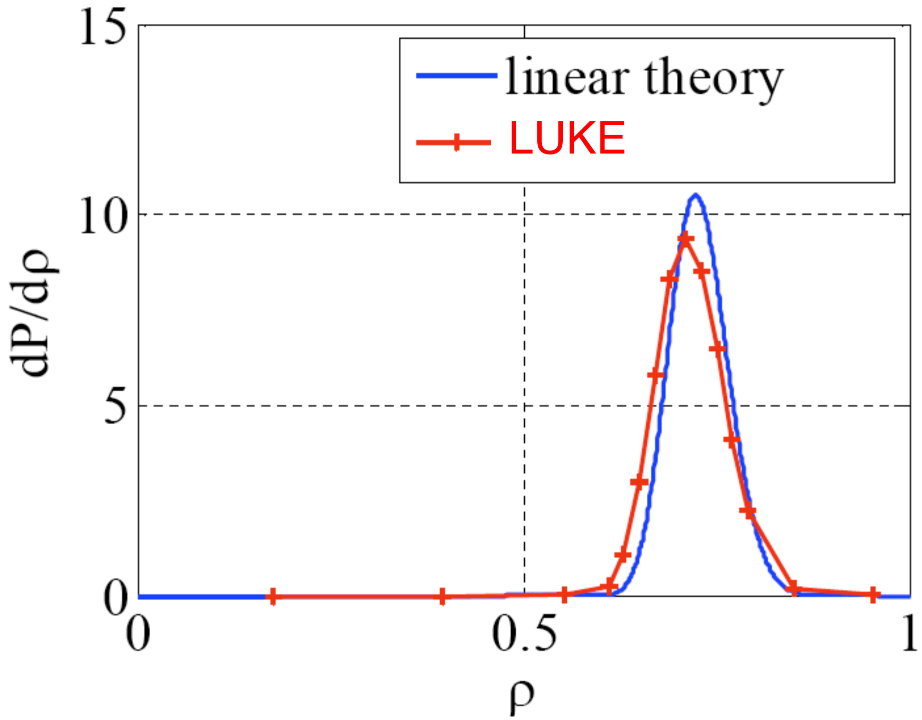

Accuracy ~ 1A/1W level

LH current drive simulations: the spectral gap problem

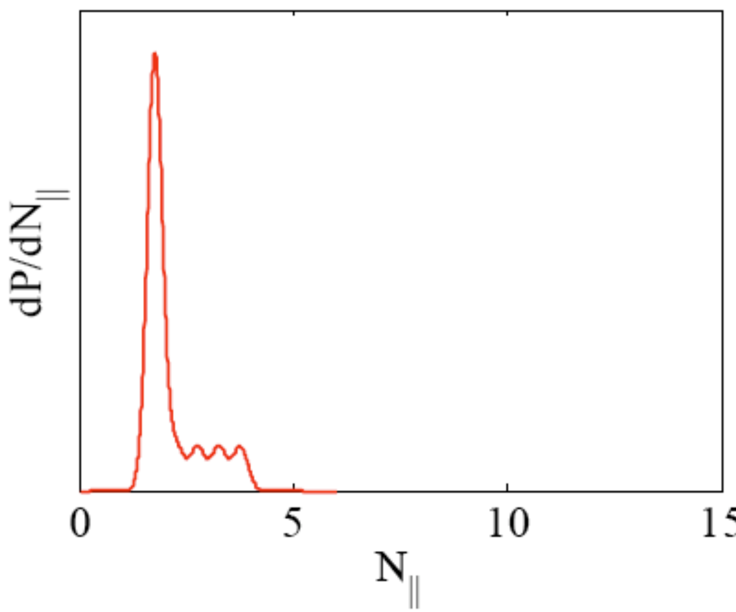

$$\frac{V_{\parallel res}}{c} = \frac{1}{N_{\parallel}}$$

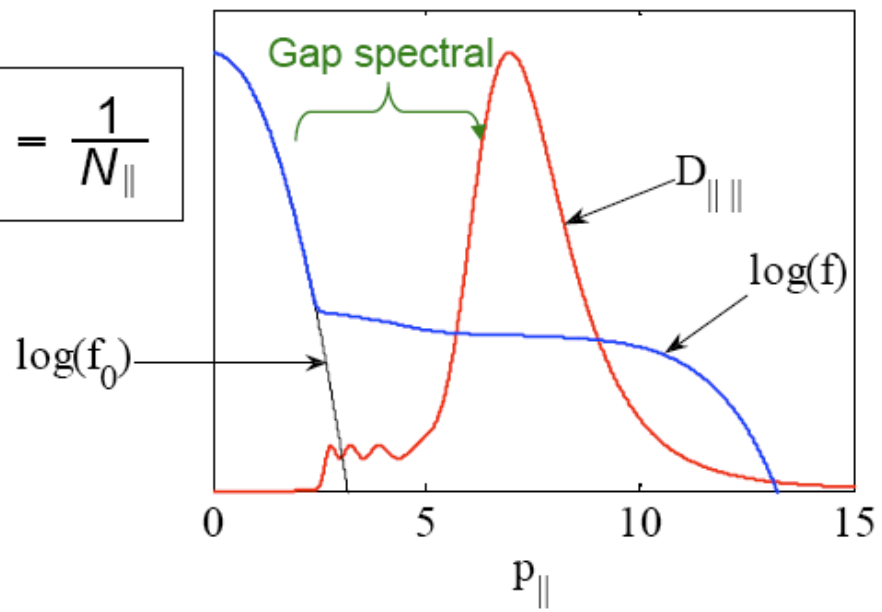

The **spectral gap** is bridged by a small fraction of the LH power at high $n_{||}$ which pulls out a tail of fast electrons from the bulk which itself contributes to absorb the remaining part of the power at low $n_{||}$ *(toroidal mode coupling by refraction)*

Lower Hybrid current drive in ITER: code benchmarking

Scen IV

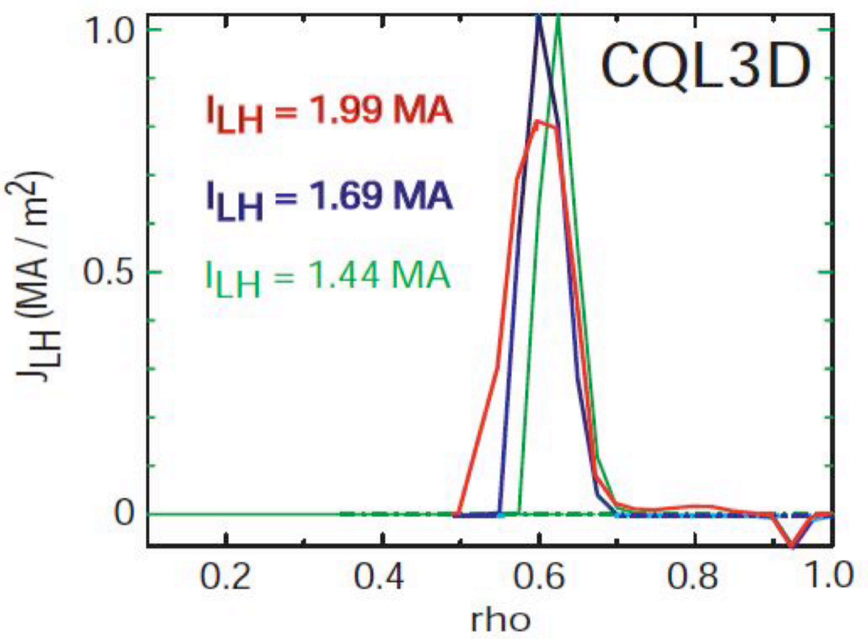

GENRAY - CQL3D: 80 rays

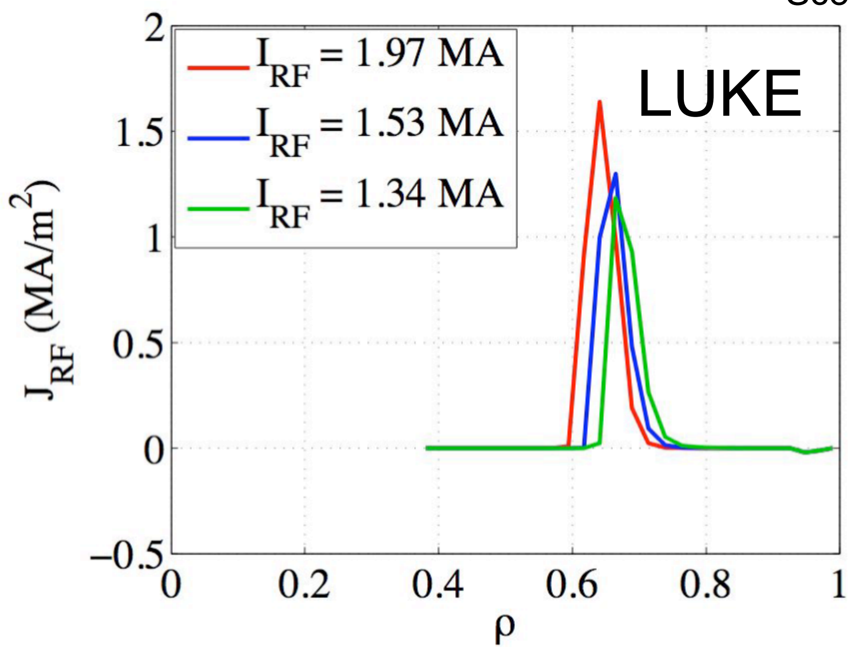

C3PO - LUKE: 3 rays

- $n_{||} = 1.9$
- $n_{||} = 2.0$
- $n_{||} = 2.1$

$$v_{||}/c \propto 1/n_{||}$$

Consistent with Fisch's theory

P_{LH} = 30 MW
Directivity = 0.87

Bonoli, P. T. et al., Proc. of the 21st IAEA Conference, Chengdu, **2006**

Lower Hybrid current drive in ITER

Scen IV

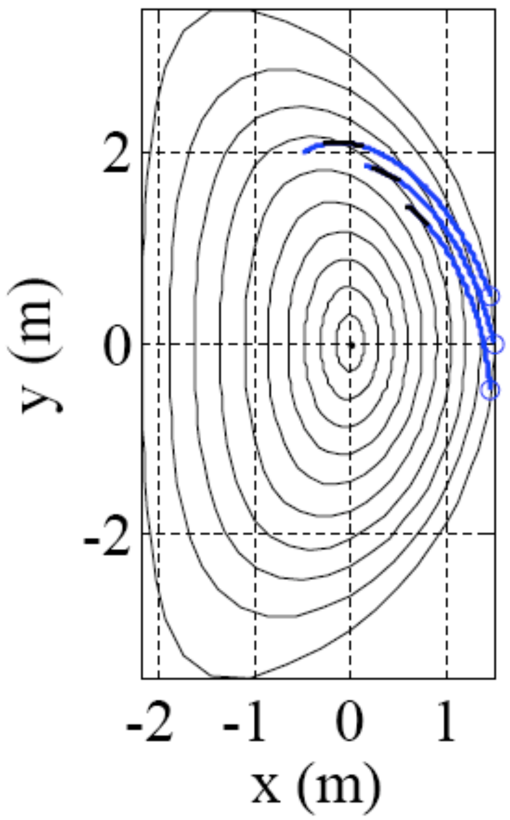

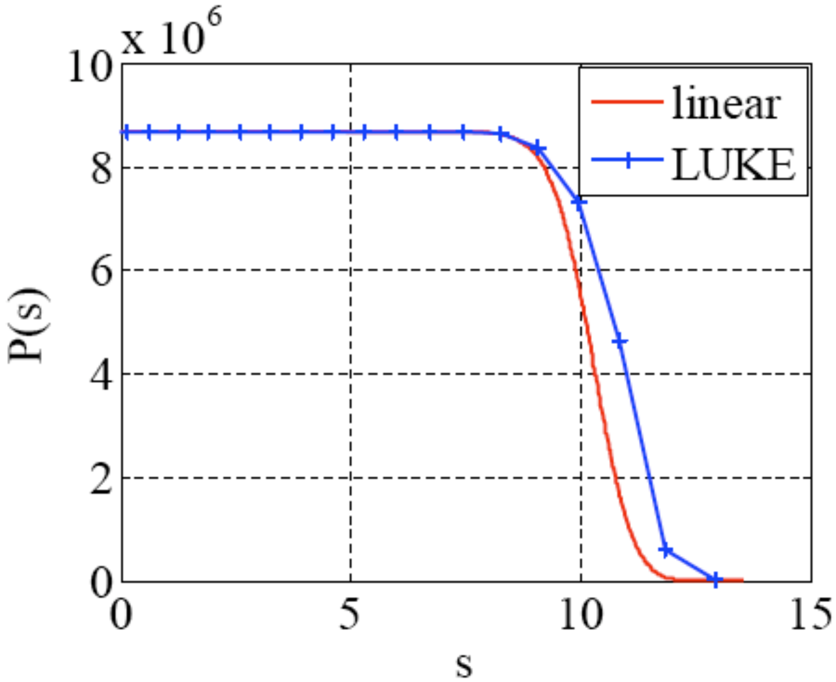

Almost linear single pass absorption gives: results independent of the number of rays !

J. Decker, Y. Peysson et al., Nucl. Fusion, 2011, 51, pp. 073025

LHCD in ITER with PAM launcher
Current drive efficiency, localization

P_{LH} = 20 MW
Directivity (**PAM**) = 0.70

Even in ITER, weak LH absorption damping may occurs at low $N_{\parallel 0}$: ray stochasticity → limit of the ray tracing model

- $N_{\parallel 0(opt)}$ = -1.85 @ 5 GHz
- Single pass absorption for $|N_{\parallel 0}|$ > 1.85
- Narrow deposition profile @ ρ ≥ 0.67

$$\eta_{opt} = \frac{1.25}{|N_{||}|^{2.5}} \times d \simeq 0.19 \times 10^{20} A.m^{-2}W^{-1}$$

Reduction by ~25% because of trapped particles

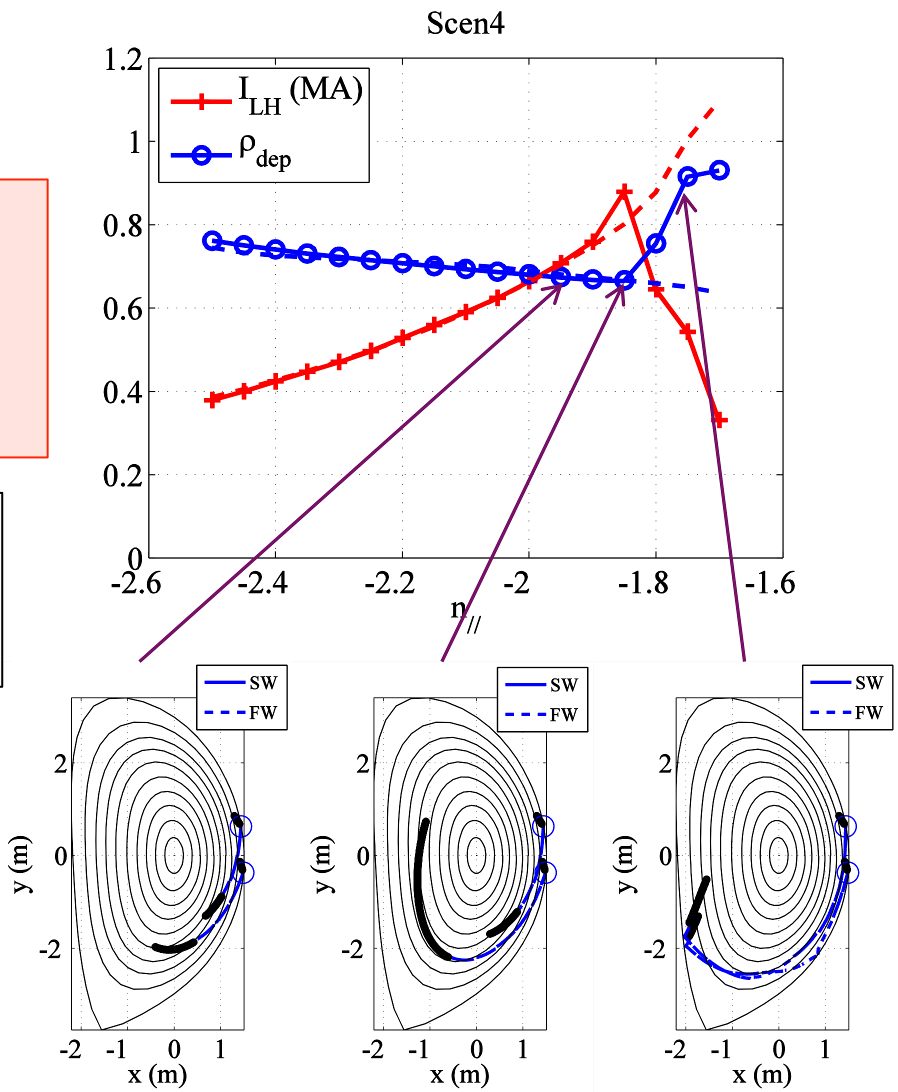

J. Decker, y. peysson, et al., Nucl. Fusion, 2011, 51, pp. 073025

LHCD in ITER
Quasilinear effects with the power level

$N_{\parallel 0(opt)} = -1.85$ @ 5 GHz

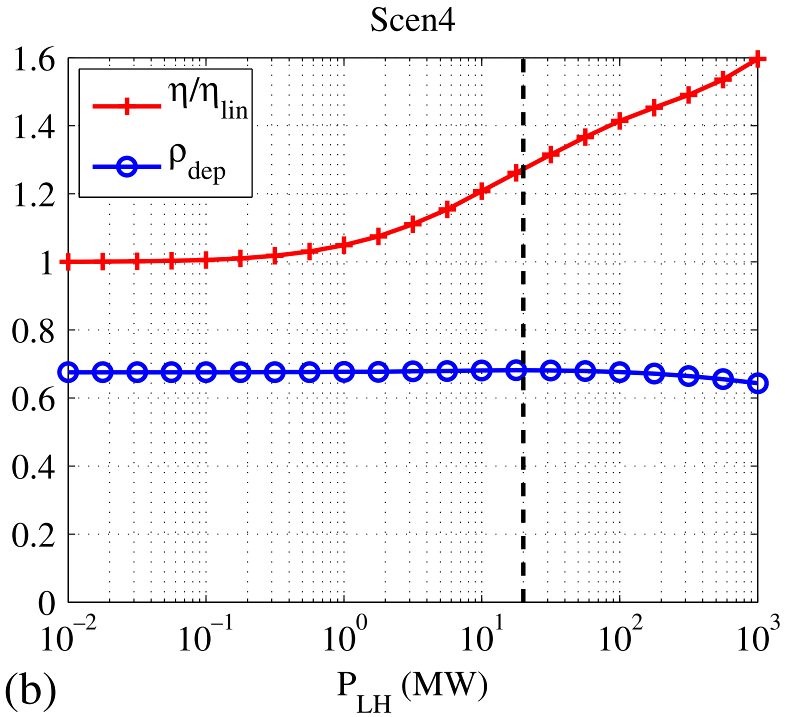

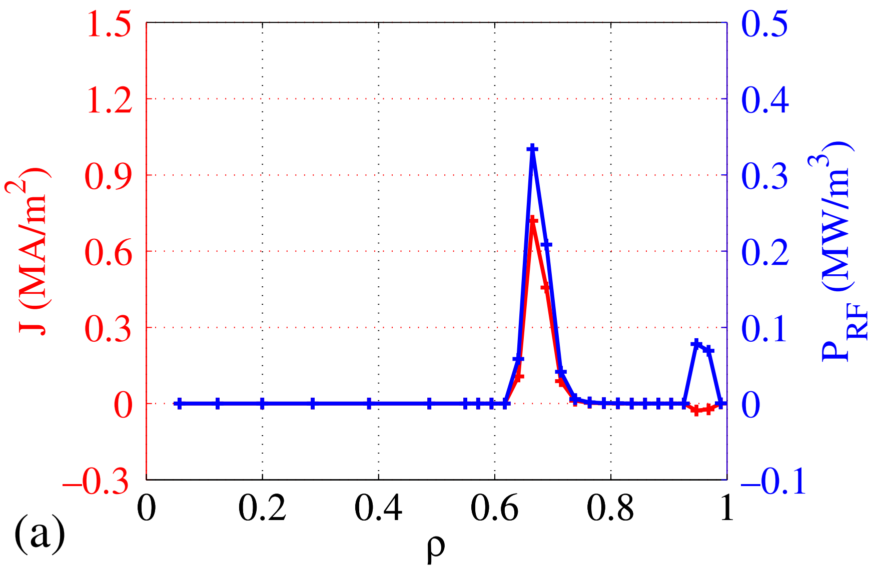

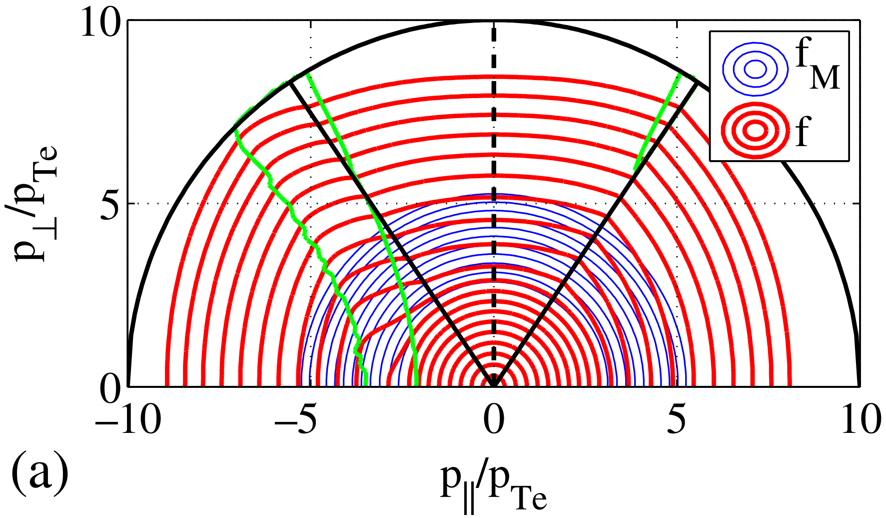

Far from the quasilinear saturation
(flat plateau in the distribution)

J. Decker, y. Peysson et al., Nucl. Fusion, 2011, 51, pp. 073025

Lower Hybrid current drive in Tore Supra
Record steady-state operation

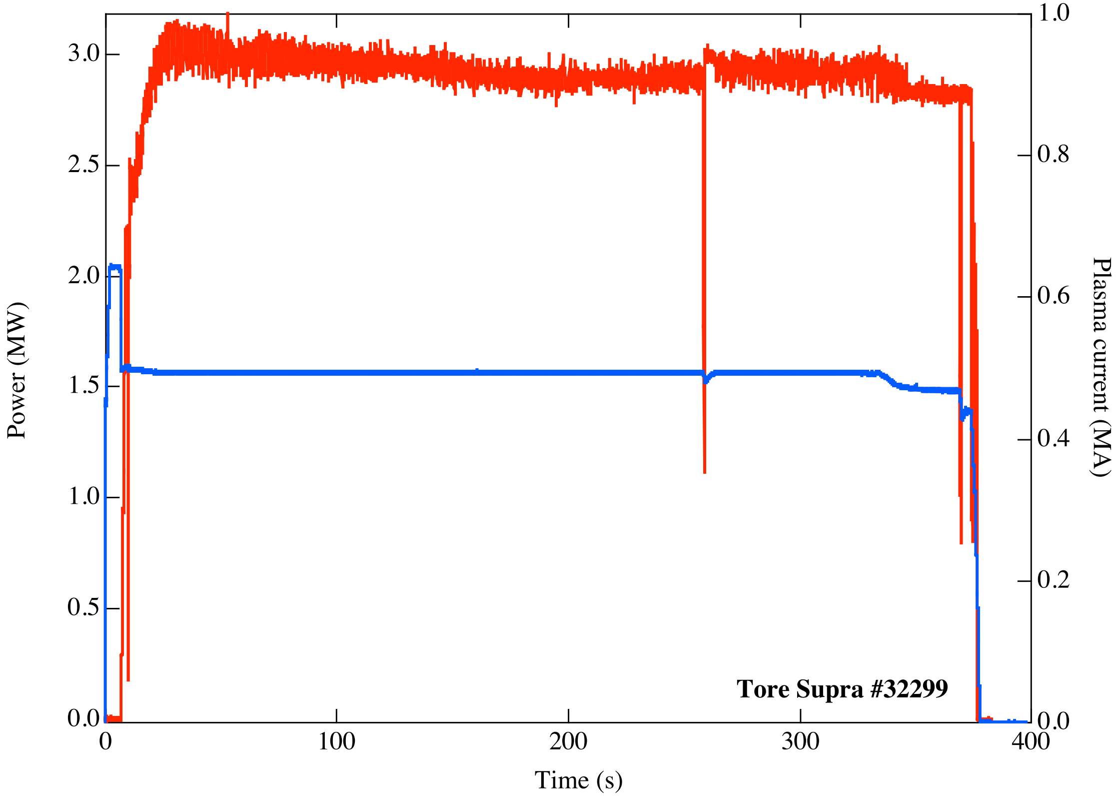

- Full LHCD (6 min.)
- 2 antennas
- $n_{||0}$ =1.7 ± 0.2
- P_{lh} = 3 MW
- directivity: 0.6 & 0.7

*Peysson, Y. and Decker, J., Theory of Fusion Plasmas, AIP Conf. Proc., **2008**, 1069, 176-187*

Lower Hybrid current drive in Tore Supra
Fast electron bremsstrahlung

Δk = 60-80 keV

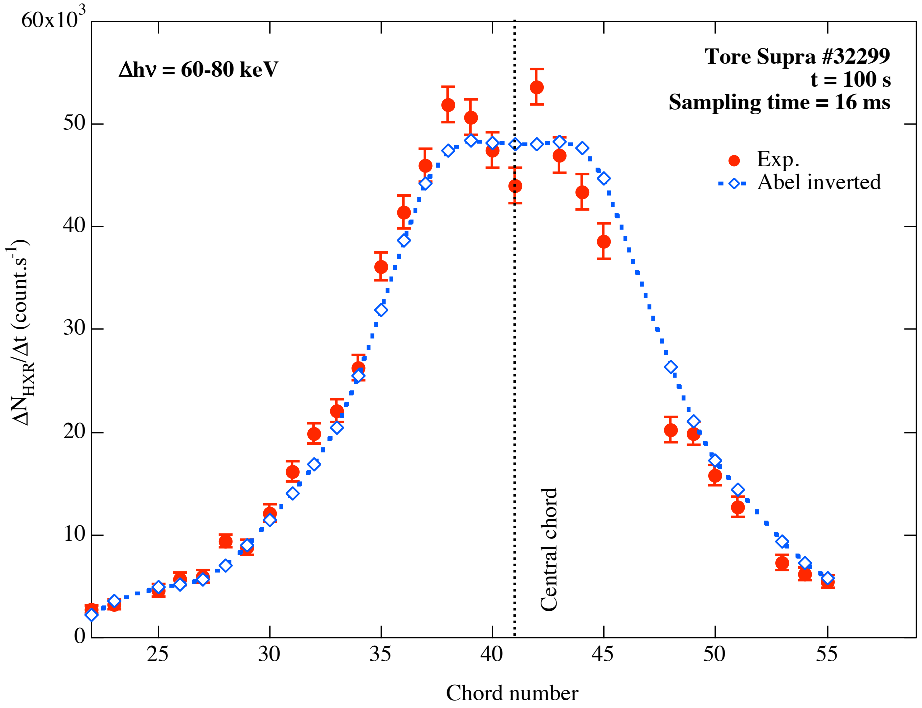

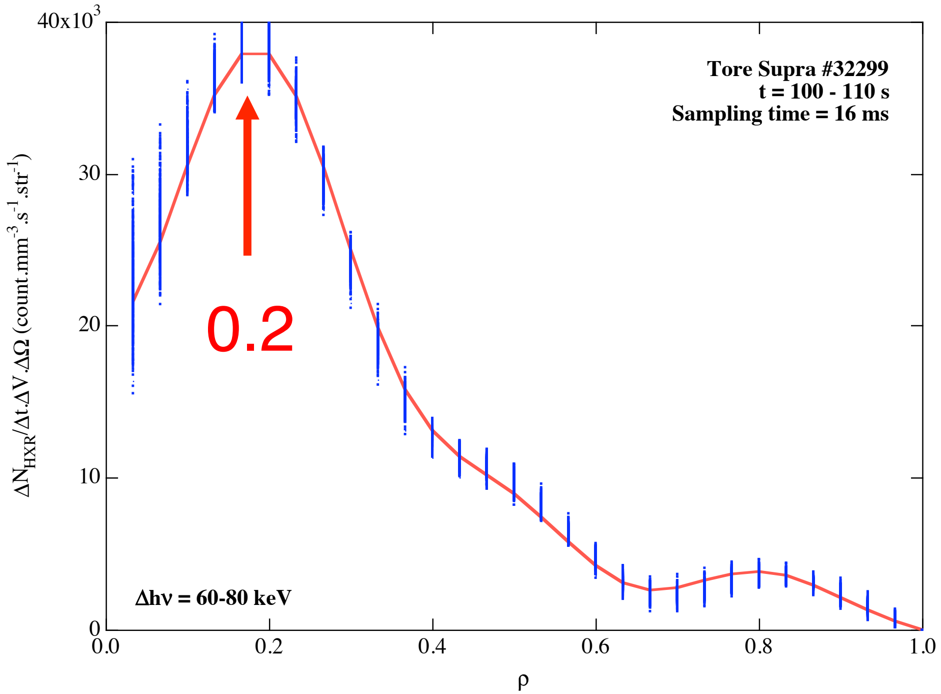

Line-integrated profile

Abel inverted profile

Very quiescent HXR profiles

*Peysson, Y. & Decker, J., Theory of Fusion Plasmas, AIP Conf. Proc., **2008**, 1069, 176-187*

Lower Hybrid current drive in Tore Supra: weak absorption regime

Tore Supra #32299

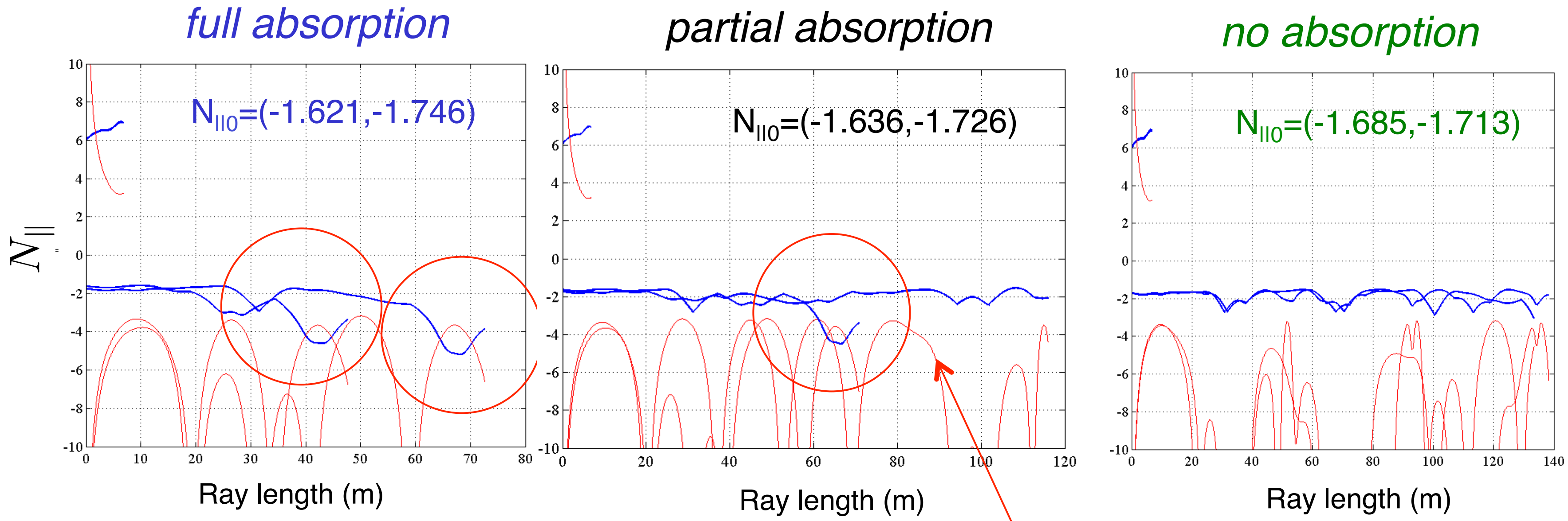

$$\frac{6.5}{\sqrt{T_e}} \propto v_\phi = 3 - 4 \times v_{th}$$

Lack of robustness of LH current drive simulations in the multipass absorption regime (most present day tokamaks) when the spectral gap is bridged by toroidal $N_{||}$ upshift → Simulations often done well beyond code validity: *ray stochasticity develops before power absorption.*

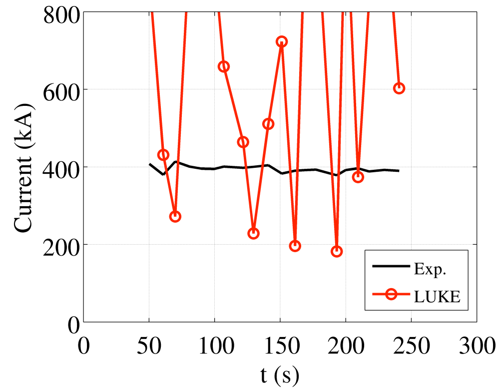

Y. Peysson, J. Decker, et al. PPCF, 53 (2011) 124028)

Full electron cyclotron current drive in TCV

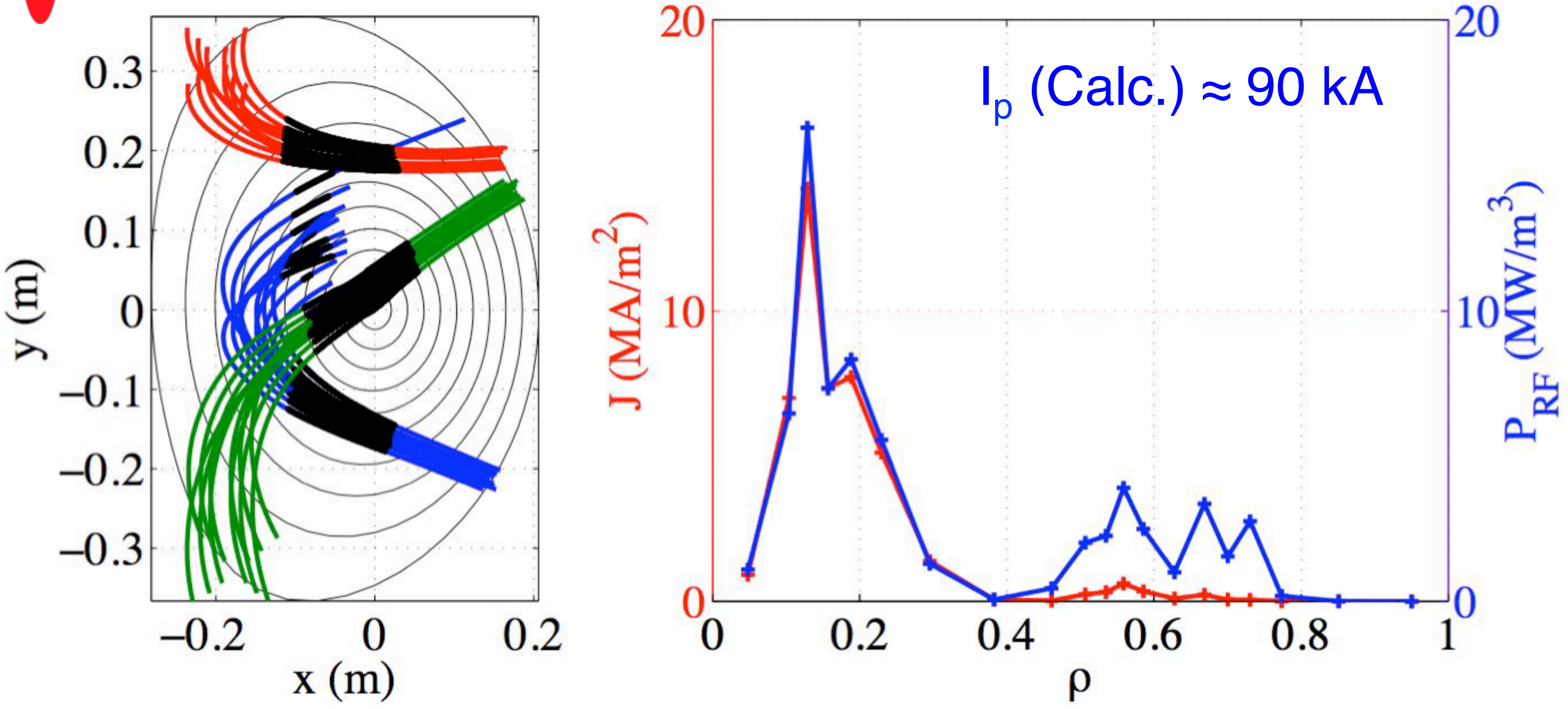

I_p (Exp.) ≈ 100 ± 10 kA

Peysson, Y. & Decker, J., Theory of Fusion Plasmas, AIP Conf. Proc., ***2008****, 1069, 176-187*

Integrated modeling of an ITB discharge with high bootstrap fraction

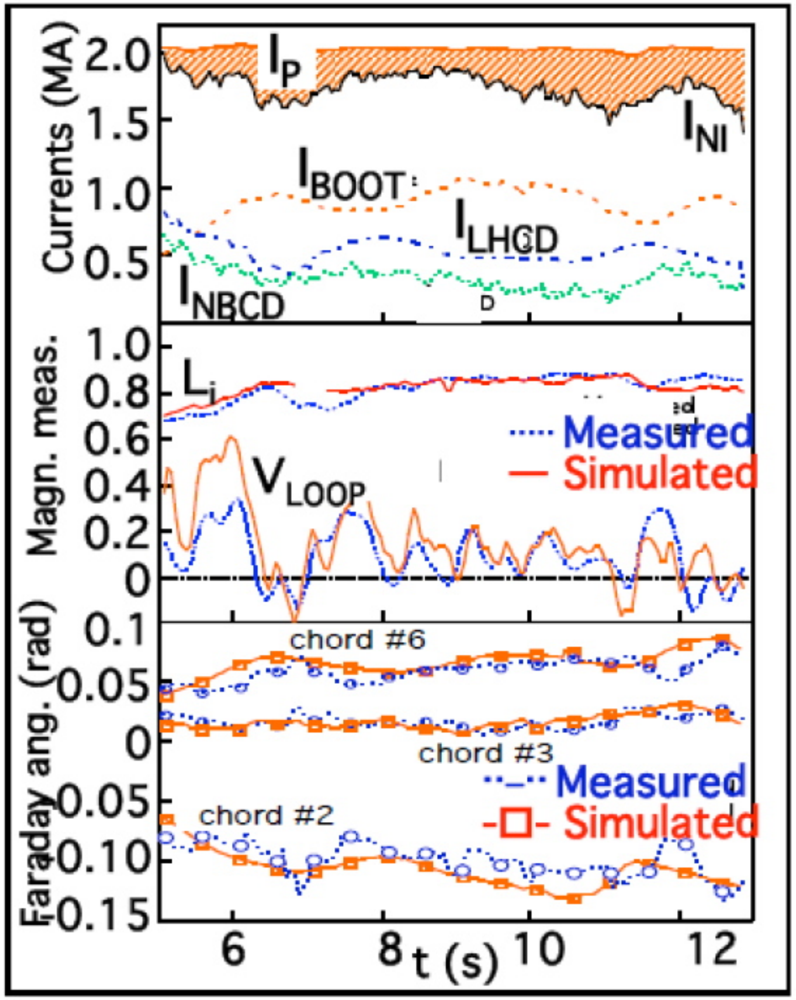

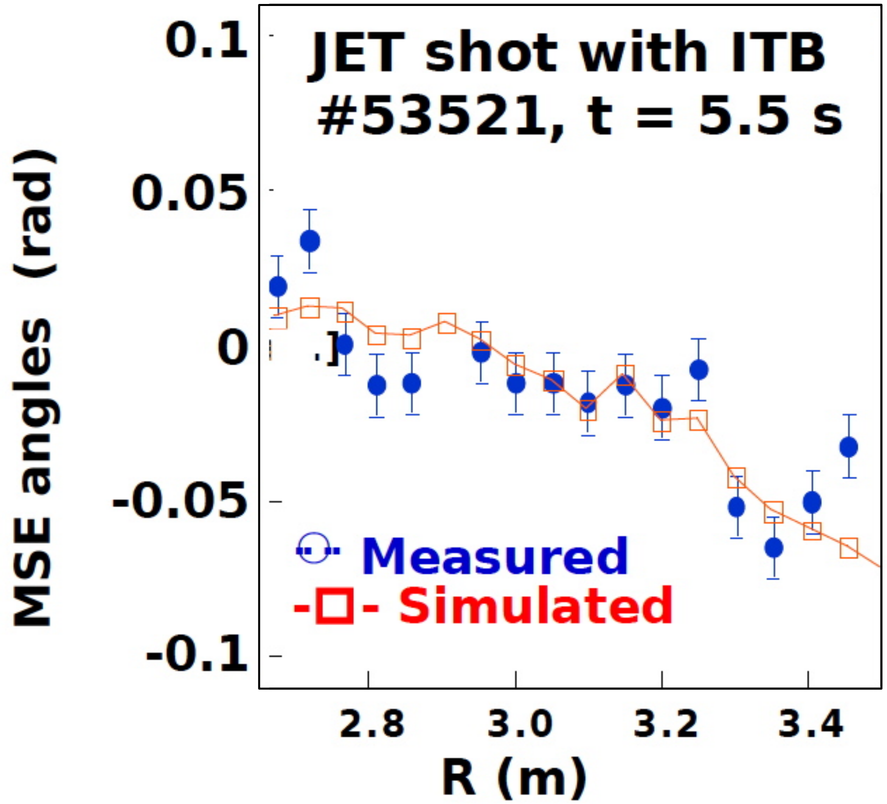

X.Litaudon et al., Nucl. Fusion 44 (2002)

Advanced studies

Influence of plasma fluctuations on rf current source

(TCV, ITER)

EC wave and edge density fluctuations

- Control of Neoclassical Tearing Modes (NTM) requires very localized EC current drive
- Edge density fluctuations → broadening of the EC current density profile

(C. Tsironis et al., Phys. Plasmas **16** (2009) 112510)
(K. Hizanidis et al., Phys. Plasmas **17** (2010) 022505)
(N. Bertelli et al., Journal of Physics: Conference Series **260** (2010) 012002)

Absorption zone

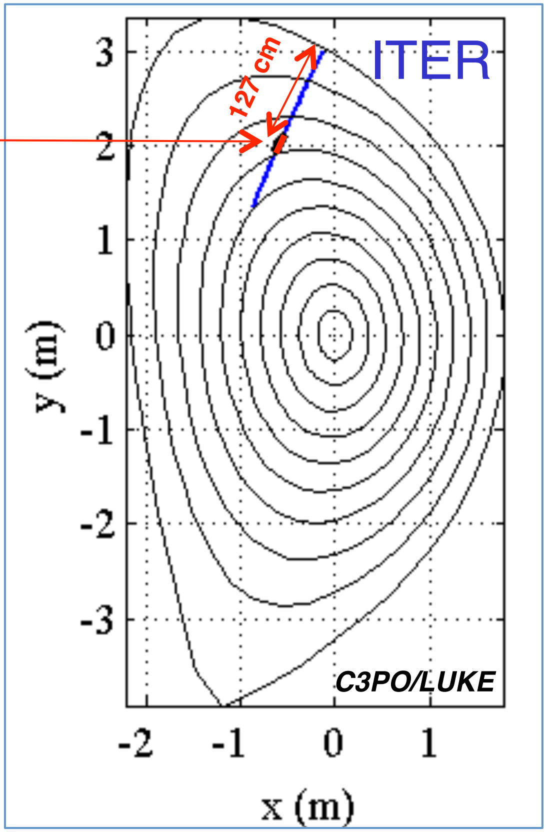

ELMy H-mode ITER scenario
EC wave: O-mode @ 170 GHz

$W_{3/2} \approx 7$ cm + ray length ≈ 127 cm

A small deviation of the rays at the plasma edge → misalignment of the RF power absorption with the island.

(R. Prater et al., Nucl. Fusion, 2008, 48, pp. 035006)

Density fluctuations and wave refraction

n_e

$$X_\perp^{sC} \equiv X_{xx}^{sC} = X_{yy}^{sC} = -\frac{\boxed{\overline{\omega}_{ps}^2}}{1-\boxed{\overline{\omega}_{cs}^2}}$$

$$X_\parallel^{sC} \equiv X_{zz}^{sC} = -\boxed{\overline{\omega}_{ps}^2}$$

$$X_\times^{sC} \equiv iX_{xy}^{sC} = \frac{\boxed{\overline{\omega}_{ps}^2}\boxed{\overline{\omega}_{cs}}}{1-\boxed{\overline{\omega}_{cs}^2}}$$

B

$$\overline{\omega}_{ps} = \omega_{ps}/\omega \qquad \omega_{ps} = \sqrt{q_s^2 \boxed{n_s}/\varepsilon_0 m_s}$$

$$\overline{\omega}_{cs} = \omega_{cs}/\omega \qquad \omega_{cs} = q_s \boxed{B_0}/m_s$$

$\boxed{\left(\overline{\omega}_{pe}^2, \overline{\omega}_{ce}^2\right) \gg 1}$ $\longrightarrow$ refraction effects are large (LH)

$\boxed{1-\overline{\omega}_{ce}^2 \ll 1}$ $\longrightarrow$ amplification by magnetic field (LH,EC)

O-mode
170 GHz

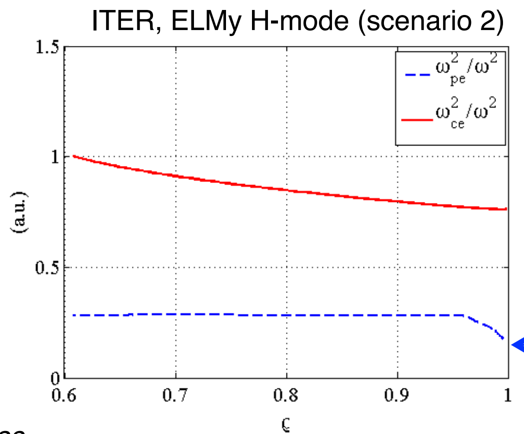

$$\boxed{\frac{1}{1-\overline{\omega}_{ce}^2} \sim 4}$$

pedestal

$$\boxed{\begin{array}{c}\delta\mathbb{X}/\mathbb{X} \\ \dfrac{\nabla_{\perp,\parallel}\delta\overline{\omega}_{pe}}{\overline{\omega}_{pe}}\end{array}}$$

Y. Peysson, et al. PPCF, 53 (2011) 124028

Electron density fluctuation model

- *Fluctuations* → time-dependent perturbation of the toroidal MHD equilibrium with a characteristic correlation time τ_f
- The spatial structure of the perturbation is described by a linear superposition of independent modes → *gyrokinetic calculations, MHD*
- Conditions for a statistical description of the fluctuations are considered → $\tau_f \ll \Delta t$
- The spatial perturbation is deduced either from a prescribed autocorrelation function or from the Wiener-Kintchine theorem knowing the power spectrum → *experiments*

Y. Peysson, J. Decker, et al. PPCF, 53 (2011) 124028

Calculation of the rf current source in presence of density fluctuations

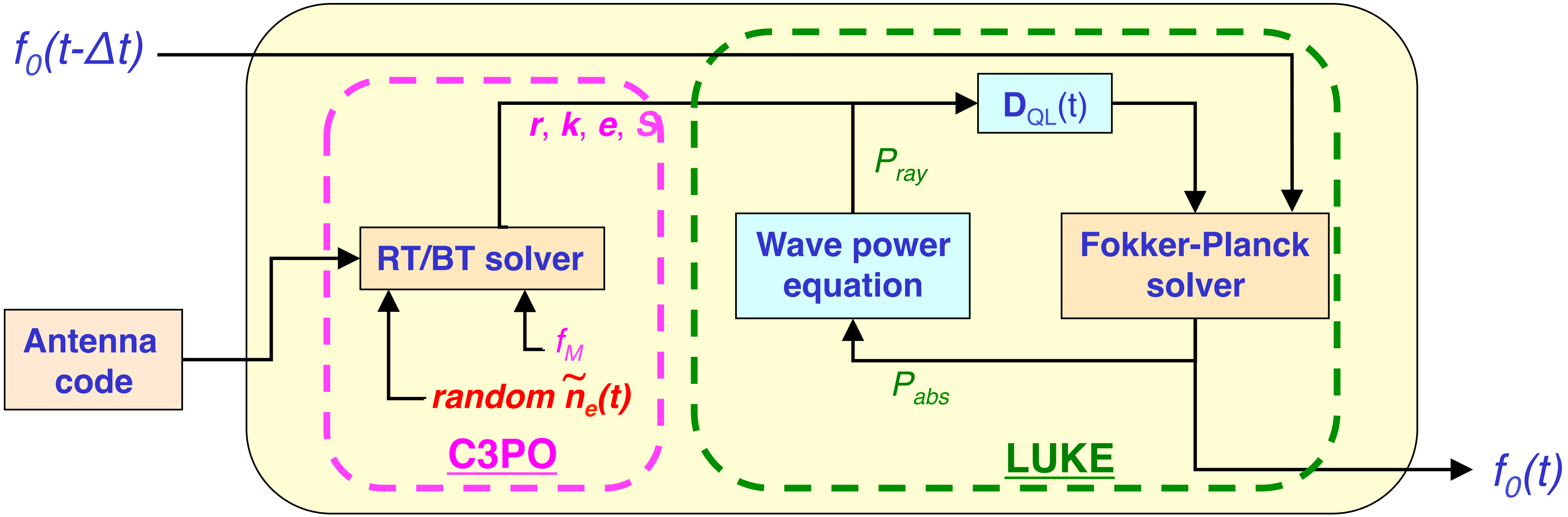

(J. Decker and Y. Peysson, Euratom-CEA, 2004, report, EUR-CEA-FC-1736)

Fluctuations far from the place where RF waves are absorbed

- time-dependent density perturbation → propagation code
- kinetic self-consistency → time evolution of f_0

Y. Peysson, J. Decker, et al. PPCF, 53 (2011) 124028

3-D ray tracing for the LH wave with electron density fluctuations (C3PO)

LH wave, 3.7 GHz

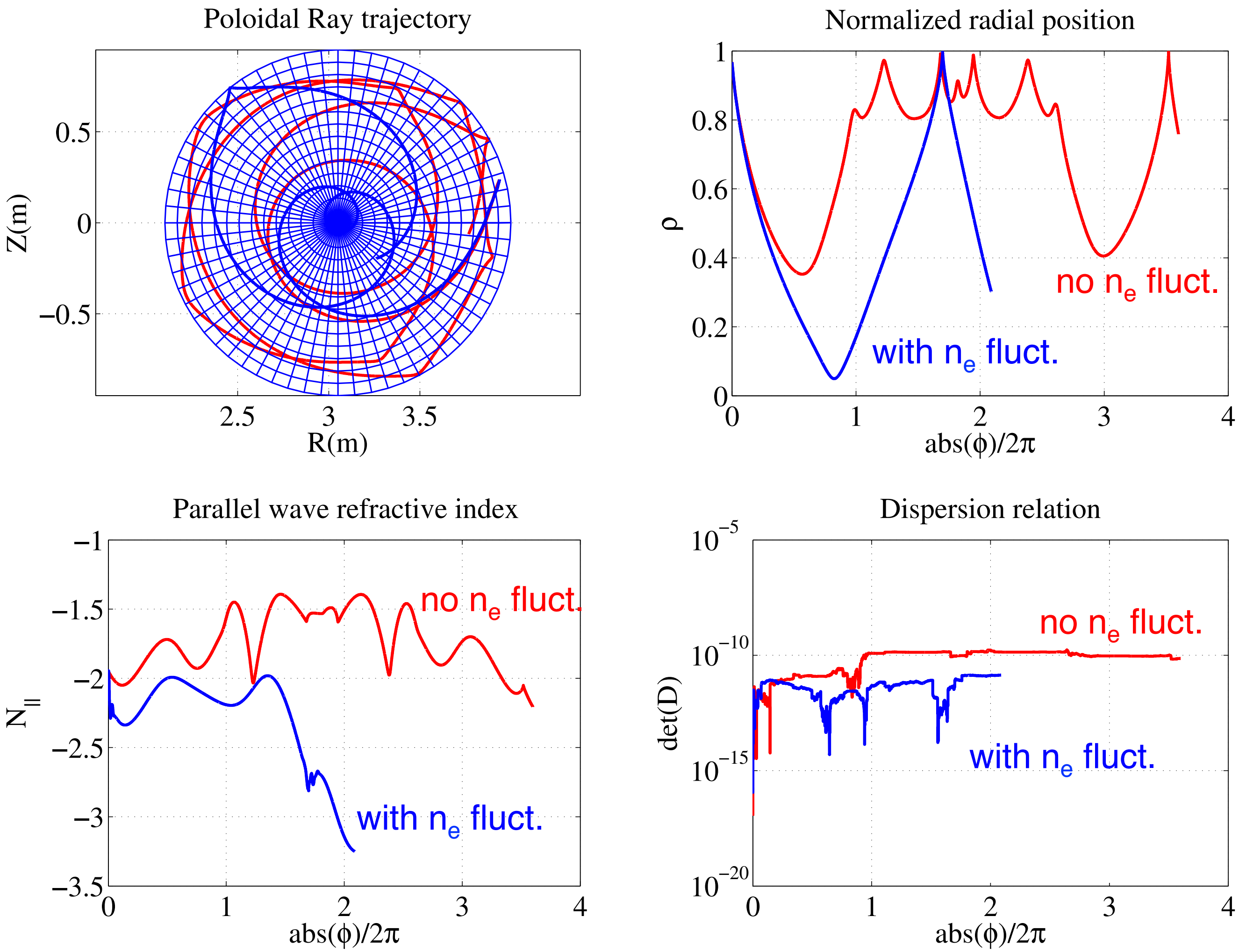

vectorized magnetic equilibrium
+
analytic description of density fluctuations

Fast and accurate calculations even with density fluctuations

+

WKB approx.

$$\nabla \widetilde{\Phi}_{l,m,n} \leq \mathbf{k}$$

Y. Peysson, J. Decker, et al., PPCF, 54 (2012) 045003

Thin fluctuating layer model (electron drift wave)

- density fluctuations driven by electron drift wave
- localization at the plasma edge
- ballooning effect (LFS/HFS amplitude)

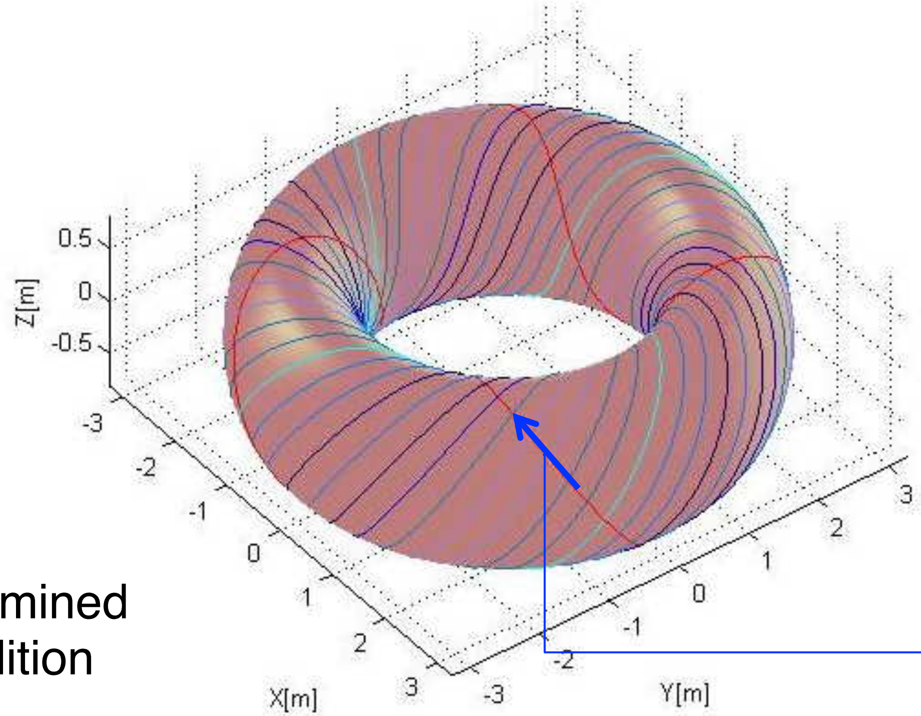

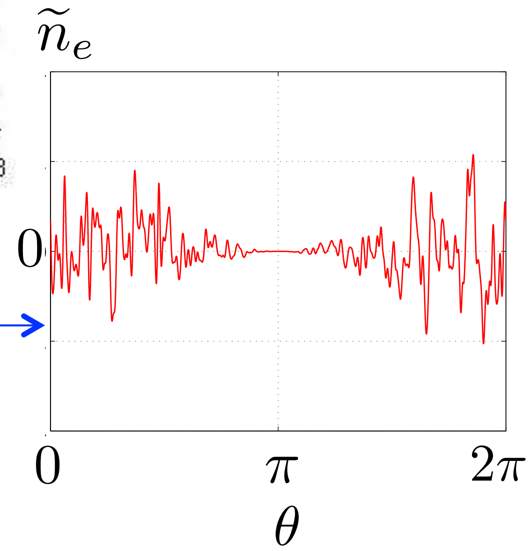

The phase is determined from the local condition

$$\boxed{\widetilde{k}_{\parallel} = 0}$$

W. Horton, Review of Modern Physics, 1999, 71, 3, pp. 735 – 778

Y. Peysson, et al. PPCF, 53 (2011) 124028

Electron Cyclotron Current Drive

- TCV, fully non-inductive discharge ECCD, I_p = 150 kA, $P_{EC} \approx$ 1.3 MW, X2-mode, three launchers, λ = 0.1, ξ_f = 1 cm, 1000 modes, $\sigma_f \equiv \tilde{n}_e/n_e$ = 1.0 et $\Delta = 0.01 a_p$ (size of the fluctuating region).

$$\boxed{\tau_f \nu_{coll} \sim 0.14}$$

- ITER, ELMy H-mode scenario: P_{EC} = 20 MW, I_{EC} = 180 kA, O-mode @ 170 Ghz, λ = 0.1, ξ_f = 1 cm, 1000 modes, scan $\sigma_f \equiv \tilde{n}_e/n_e$ and Δ (size of the fluctuating region).

$$\boxed{\tau_f \nu_{coll} \sim 0.44}$$

Density fluctuations broaden the EC driven current

TCV, #18532, $I_{exp} \approx 150$ kA, full ECCD

no fluctuation

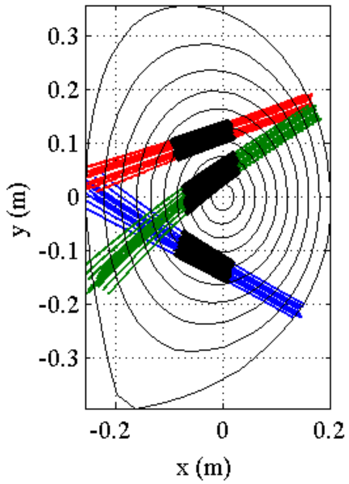

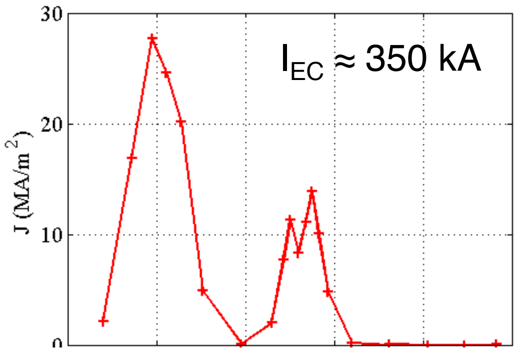

with fluctuations
$\tilde{n}_e/n_e \approx \sigma_f = 1.0$
$\Delta = 0.01a_p$
$\lambda = 0.1$
$\xi_f = 1$ cm
1000 modes

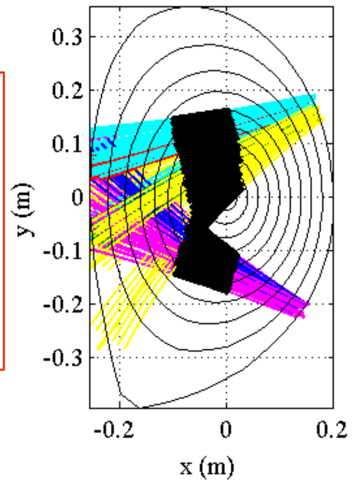

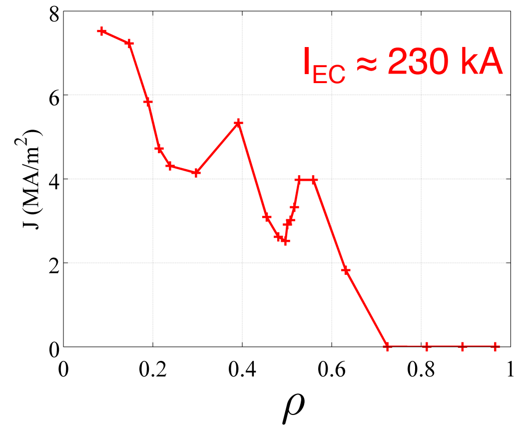

Y. Peysson, et al. PPCF, 53 (2011) 124028

Non-thermal bremsstrahlung during ECCD in presence of fluctuations

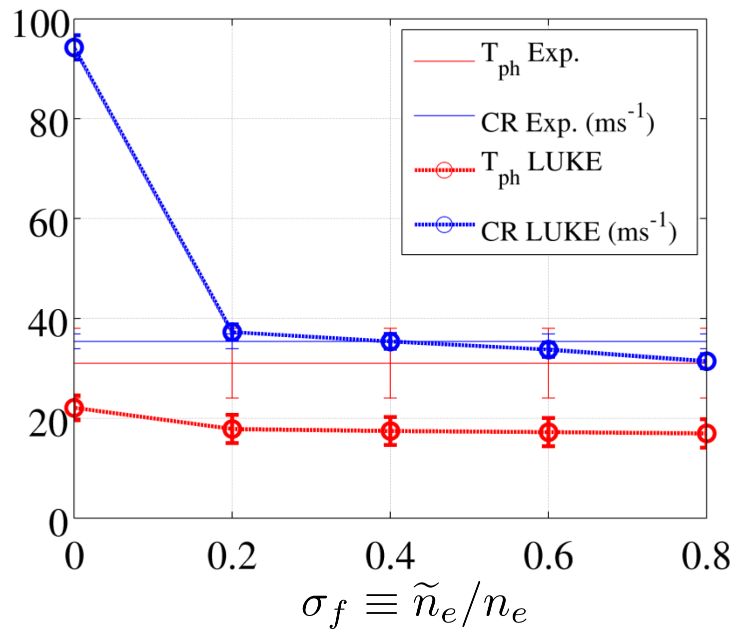

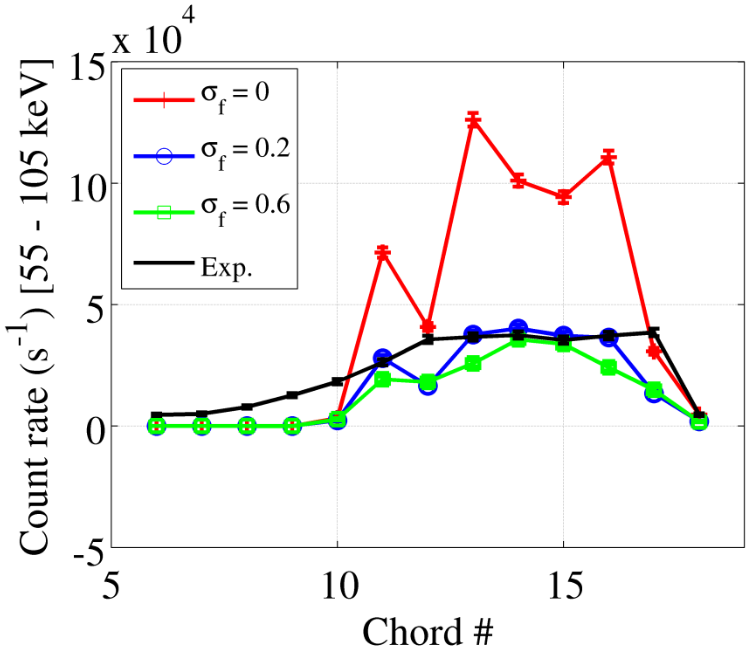

- **The reconstructed non-thermal bremsstrahlung count rate (central chord) is very close to the experimental HXR signal in the presence of fluctuations →** good match of CR versus chord number for $\sigma_f = 0.2$

- The photon temperature is fairly independent of fluctuations

J. Decker, Y. Peysson, et al., EC-17 workshop (2012) Deurne, The Netherlands

Fast electron anomalous radial transport vs density fluctuations for ECCD in TCV

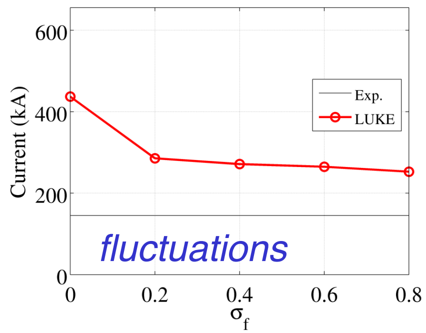

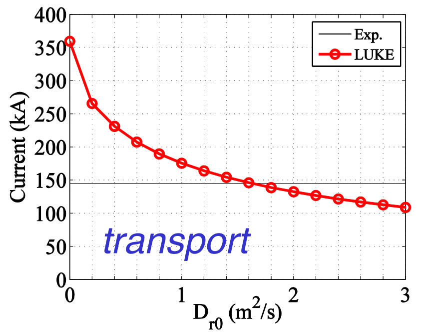

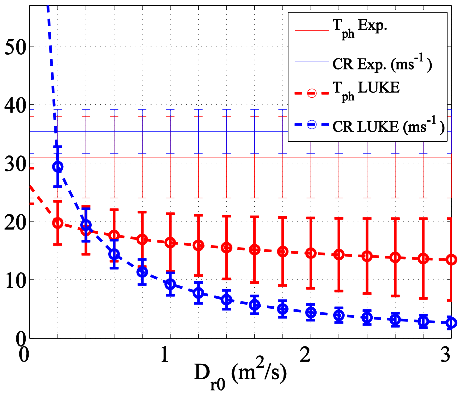

- To reduce I_{EC} by a factor 1.5 :
  - With D_{r0} = 0.4 m²/s, CR decreases by a factor 8
  - With σ_f =0.2, CR decreases by a factor 2.5
- **The underlying mechanism is different**
  - Radial transport : fast electrons are generated locally then diffuse radially while slowing down at the same time *(R.W. Harvey, et al., PRL **88** (2002) 205001; P. Nikkola, et al., NF **43** (2003) 1343)*
  - Fluctuations : the location where fast electrons are generated fluctuates

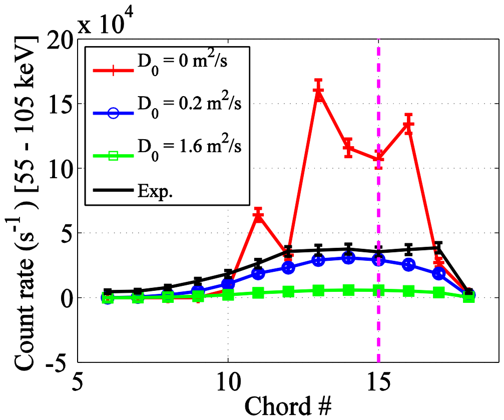

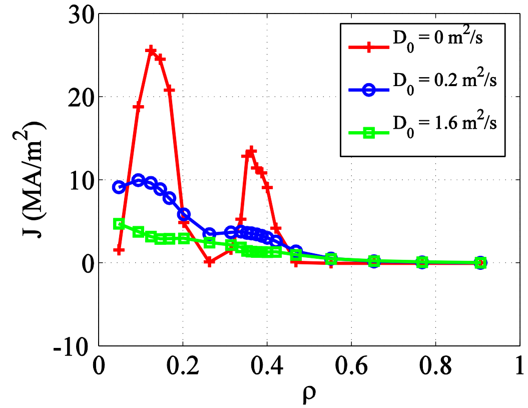

J. Decker, Y. Peysson et al., EC-17 workshop (2012) Deurne, The Netherlands

Fluctuations broaden EC current profile in ITER

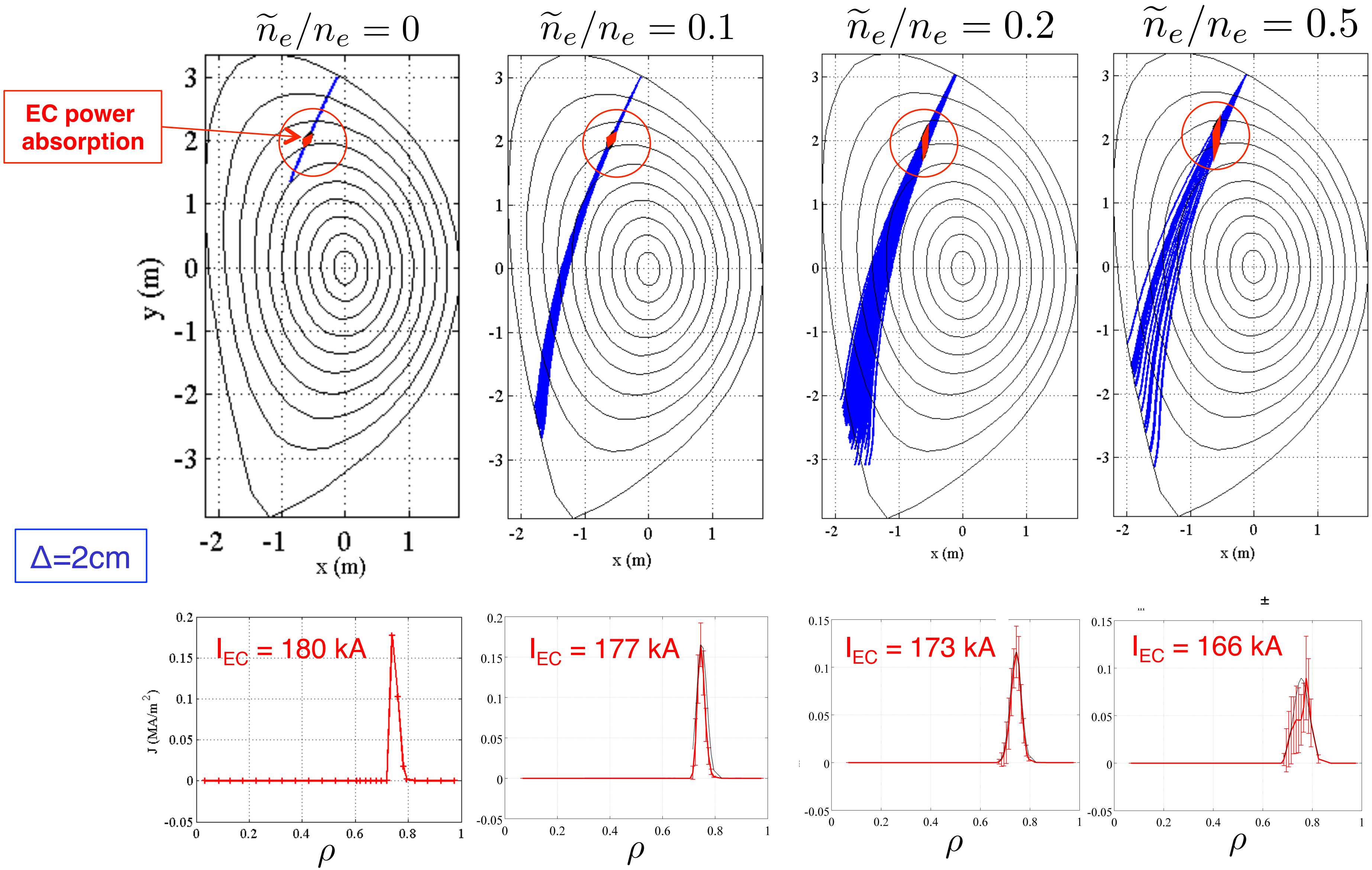

Y. Peysson, J. Decker, et al. PPCF, 53 (2011) 124028

Edge fluctuations could impact NTM stabilization in ITER

ITER, ELMy H-mode scenario, ECCD, O-mode @ 170 GHz

Fluctuating region Δ

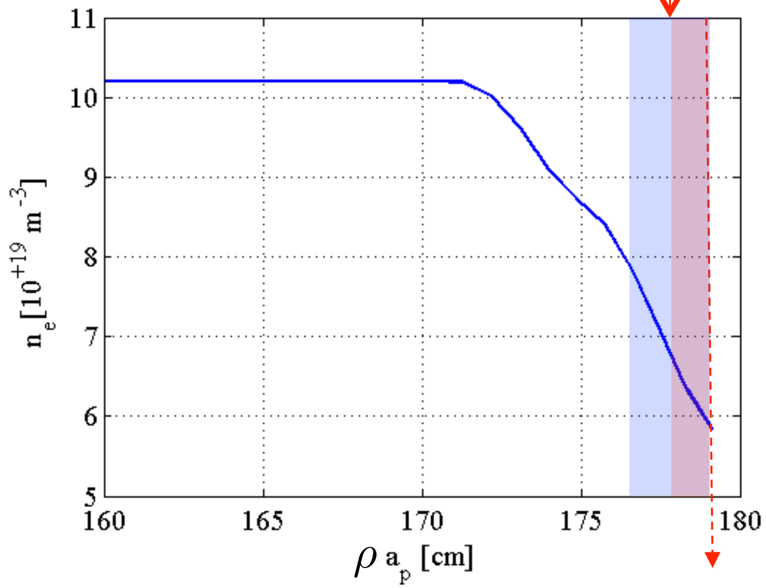

separatrix

Time-averaged EC power deposition

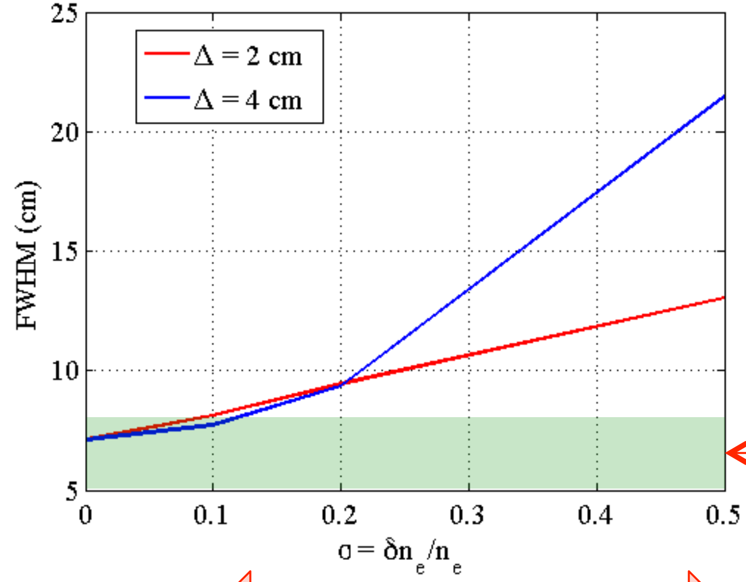

NTM island width $W_{3/2}$

(R.J. La Haye et al., Nucl. Fusion, 2006, 46, pp. 451–461)

For $\tilde{n}_e/n_e$ >> 10%, NTM stabilization in ITER by ECCD may be challenging !

Y. Peysson, J. Decker, et al. PPCF, 53 (2011) 124028

Advanced studies

Integrated modeling for designing stable MHD scenarios

(ITER)

Control of an internal transport barrier in ITER CRONOS-C3PO/LUKE

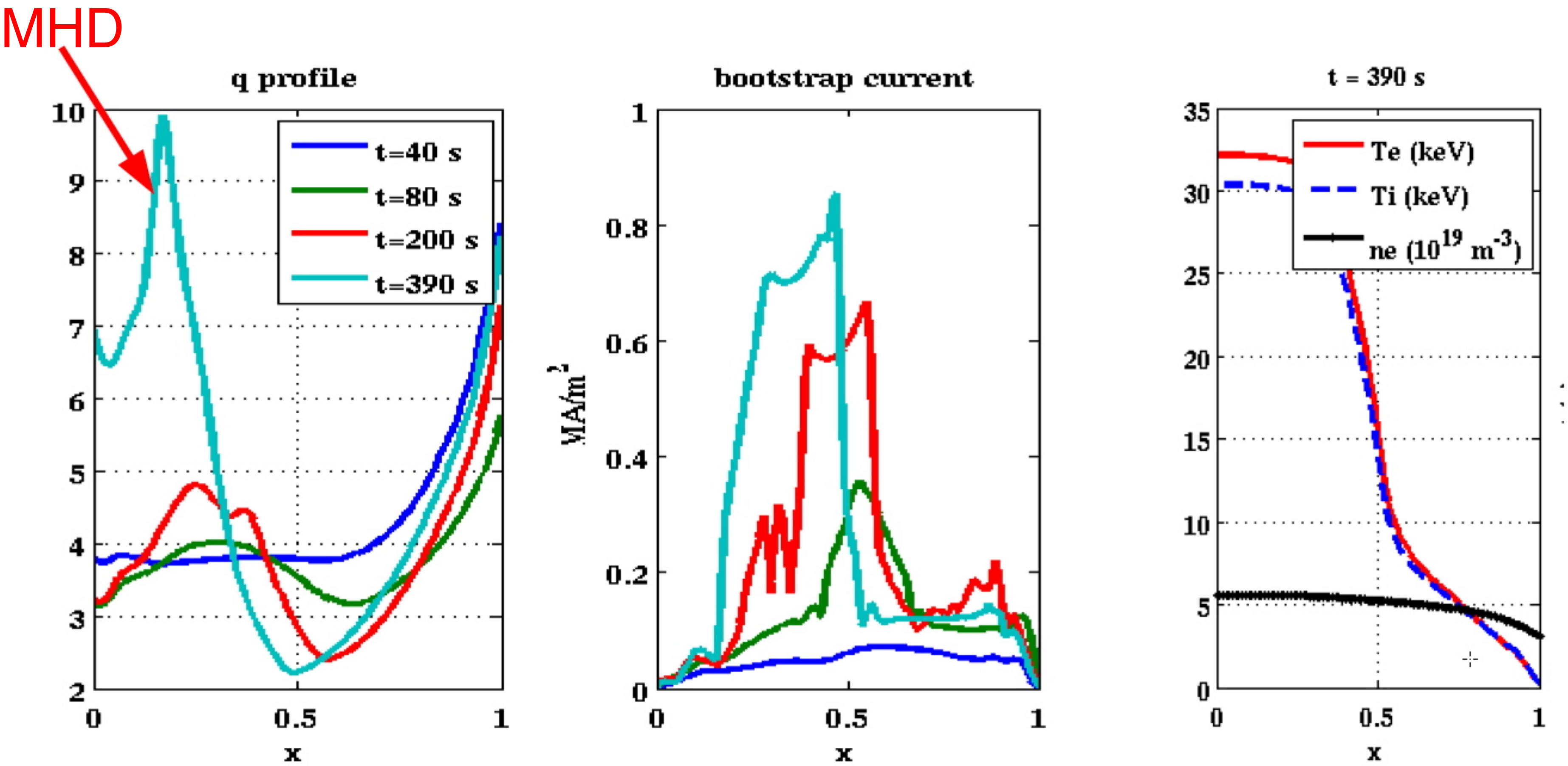

- *The internal transport barrier migrates towards the plasma center because of the misalignment between the thermal bootstrap current with the total current despite feedback control*
- *The external sources of current cannot compensate and maintain the position of the internal transport barrier*

W. Houlberg et al., Nucl. Fusion 45 (2005)

Control of an internal transport barrier in ITER CRONOS-C3PO/LUKE

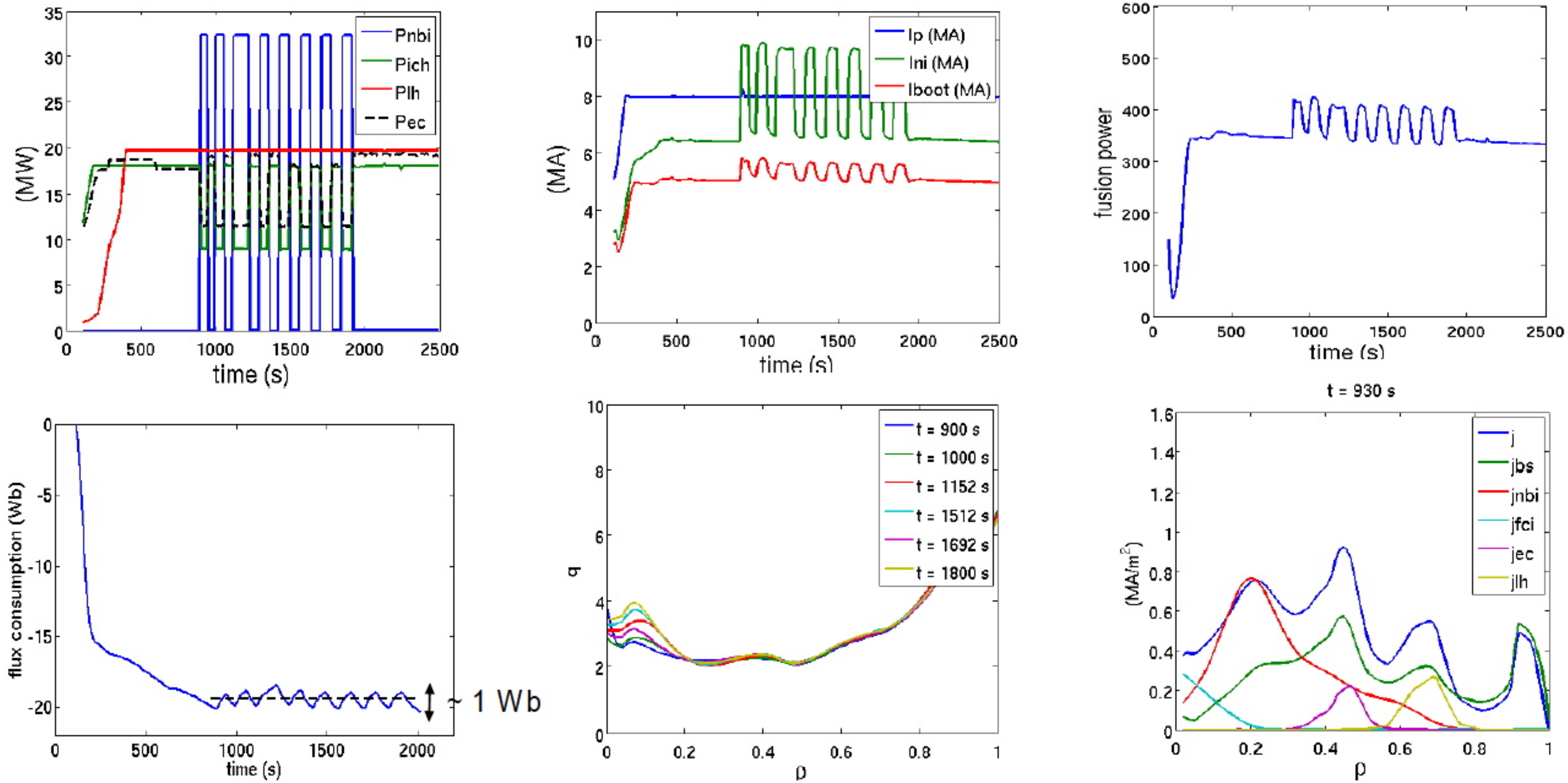

Continuous cyclic scenario solves the problem of current source alignment

J. Garcia et al., Nucl. Fusion 50 (2010) 025025

Advanced studies

Towards neoclassical current drive simulations

Neoclassical current drive calculations

Maxwellian plasma

non-Maxwellian plasma

$$j_{plasma} = \boxed{j_{configuration}} + \boxed{j_{ext.}}$$

Unified neoclassical theory for non-Maxwellian plasmas

- Exact Hamiltonian *(Lie transform)*
- Large orbits, non-local dynamics

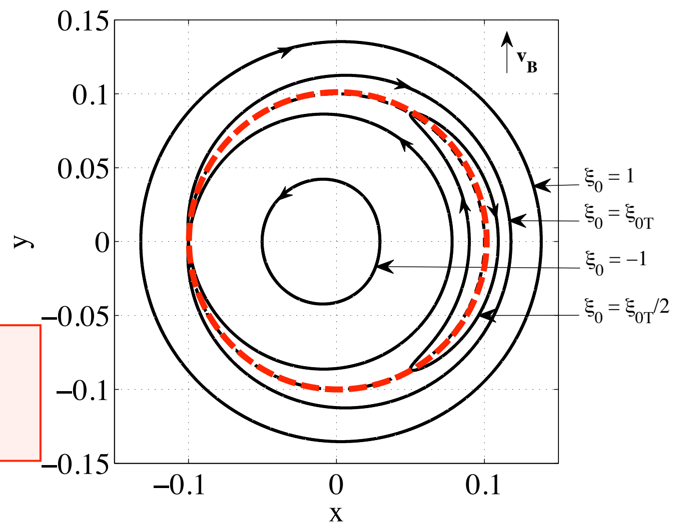

Cross-physical effects between momentum and configuration spaces dynamics (electrons, ions)

Brizard, et al.., Phys. Plasmas, 2009, 16, 10, pp. 102304

Near identity Lie transform

Derive an exact guiding-center Hamiltonian and Poisson bracket

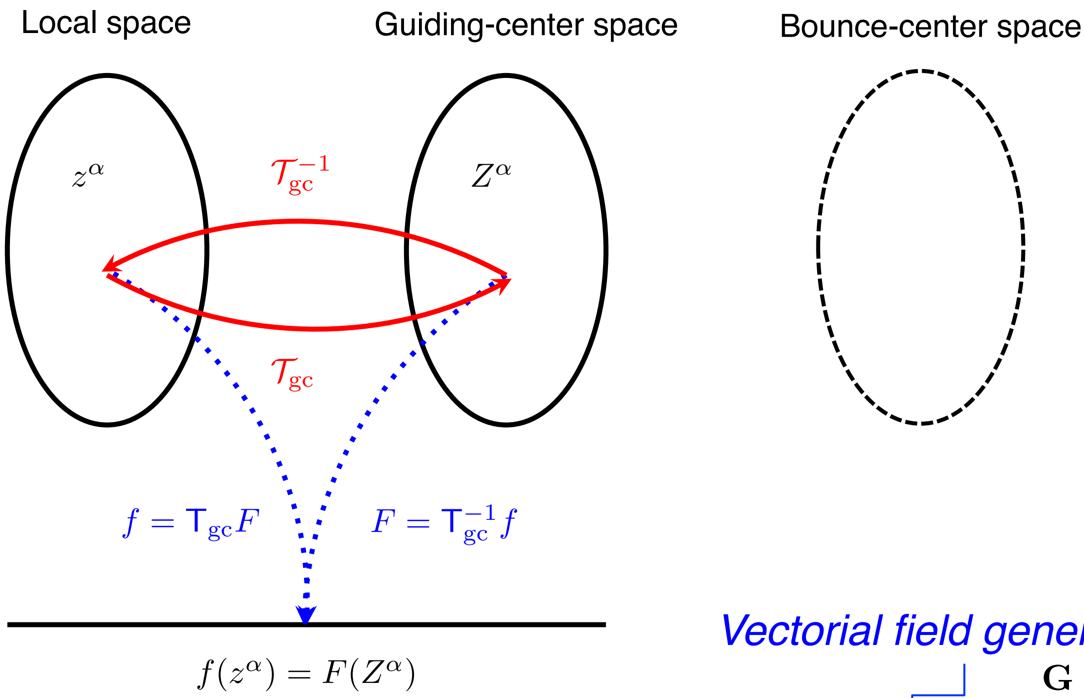

*Vectorial field generator **G***

$$\mathbf{G} \equiv G^\alpha \partial / \partial z^\alpha$$

Coordinates transformation $\quad \mathcal{T}_{\mathrm{gc}} \; : \; z^\alpha \rightarrow \overline{z}^\alpha = \exp\left(\epsilon_{\mathrm{B}} \boxed{\mathbf{G}}\right) z^\alpha$

« push-forward » transform of a Lagrangian 1-form $\quad \mathsf{T}_{\mathrm{gc}}^{-1} \; : \; \Gamma \rightarrow \overline{\Gamma} = \exp\left(-\epsilon_{\mathrm{B}} \boxed{\mathcal{L}_{\mathbf{G}}}\right) \Gamma$

*Lie derivative along **G***

Brizard, et al.., Phys. Plasmas, 2009, 16, 10, pp. 102304

Convection vector and diffusion tensor in the thin orbit approximation

$$\left\{\begin{aligned}
\mathcal{K}_{gc}^{\overline{\psi}} &= \epsilon_\psi \delta\psi \left[\nu_l + \frac{1}{\xi}\nu_t\right] + \mathcal{O}\left(\epsilon^2, \epsilon\epsilon_\psi, \epsilon_\psi^2\right) \\
\mathcal{K}_{gc}^{p} &= -\left[1 - \epsilon\lambda_{gc}\frac{1-\xi^2}{2\xi}\frac{\partial}{\partial\xi}\right]\nu_l p + \mathcal{O}\left(\epsilon^2, \epsilon\epsilon_\psi, \epsilon_\psi^2\right) \\
\mathcal{K}_{gc}^{\xi_0} &= -\frac{1-\xi_0^2}{2\xi_0}\left[\left(\epsilon_\psi\overline{\delta\psi} + \epsilon\lambda_{gc}\right)\nu_l \right. \\
&\quad \left. + \frac{2\xi}{1-\xi^2}\left(1 - \epsilon\lambda_{gc} - \epsilon\lambda_{gc}\frac{1-\xi^2}{2\xi}\frac{\partial}{\partial\xi} + \epsilon_\psi\overline{\delta\psi}\frac{1-\xi^2}{2\xi^2}\right)\nu_t\right] + \mathcal{O}\left(\epsilon^2, \epsilon\epsilon_\psi, \epsilon_\psi^2\right)
\end{aligned}\right.$$

Thin orbit approximation: $\epsilon_\psi \equiv \left(\psi - \overline{\psi}\right)/\overline{\psi} \ll 1$

Magnetic non-uniformity: $\epsilon \equiv \rho/L_B \ll 1$

$$\left\{\begin{aligned}
\mathcal{D}_{gc}^{\overline{\psi}\overline{\psi}} &= \mathcal{O}\left(\epsilon^2, \epsilon\epsilon_\psi, \epsilon_\psi^2\right) \\
\mathcal{D}_{gc}^{pp} &= \left[1 - \epsilon\lambda_{gc}\frac{1-\xi^2}{2\xi}\frac{\partial}{\partial\xi}\right] D_l + \mathcal{O}\left(\epsilon^2, \epsilon\epsilon_\psi, \epsilon_\psi^2\right) \\
\mathcal{D}_{gc}^{\xi_0\xi_0} &= \frac{1-\xi_0^2}{p^2}\frac{\xi^2}{\Psi\xi_0^2}\left[\left(1 - \epsilon\lambda_{gc} - \epsilon\lambda_{gc}\frac{1-\xi^2}{2\xi}\frac{\partial}{\partial\xi} + \epsilon_\psi\overline{\delta\psi}\frac{1-\xi^2}{\xi^2}\right) D_t \right. \\
&\quad \left. + \frac{1}{\xi}\left(\epsilon\lambda_{gc} + \epsilon_\psi\overline{\delta\psi}\right) D_\times\right] + \mathcal{O}\left(\epsilon^2, \epsilon\epsilon_\psi, \epsilon_\psi^2\right) \\
\mathcal{D}_{gc}^{p\overline{\psi}} &= -\epsilon_\psi\frac{\delta\psi}{p}\left[D_l + \frac{1}{\xi}D_\times\right] + \mathcal{O}\left(\epsilon^2, \epsilon\epsilon_\psi, \epsilon_\psi^2\right) \\
\mathcal{D}_{gc}^{p\xi_0} &= \frac{1-\xi_0^2}{2p\xi_0}\left[\left(\epsilon_\psi\overline{\delta\psi} + \epsilon\lambda_{gc}\right) D_l \right. \\
&\quad \left. + \frac{2\xi}{1-\xi^2}\left(1 - \epsilon\lambda_{gc} - \epsilon\lambda_{gc}\frac{1-\xi^2}{2\xi}\frac{\partial}{\partial\xi} + \epsilon_\psi\overline{\delta\psi}\frac{1-\xi^2}{2\xi^2}\right) D_\times\right] + \mathcal{O}\left(\epsilon^2, \epsilon\epsilon_\psi, \epsilon_\psi^2\right) \\
\mathcal{D}_{gc}^{\overline{\psi}\xi_0} &= -\epsilon_\psi\delta\psi\frac{1-\xi_0^2}{p^2\xi_0}\left[D_t + \frac{\xi}{1-\xi^2}D_\times\right] + \mathcal{O}\left(\epsilon^2, \epsilon\epsilon_\psi, \epsilon_\psi^2\right)
\end{aligned}\right.$$

Classical Maxwellian bootstrap current recovered (Lorentz collision operator)

LUKE 2: numerical algorithm of LUKE 1 preserved, but more off-diagonals elements, Jacobian modified, and the physical meaning of ξ is no more a cosine of the pitch-angle

J. Decker, Y. Peysson, et al., *Phys. Plasmas* 17, 112513 (2010)

Conclusions and prospects

Conclusions and prospects

- Simulation of rf current source is a central activity for self-consistent tokamak modeling of advanced scenario (ITER)

- Using advanced computer technology and powerful numerical algorithms *(remote computing, multicore, GPU)*, fast calculations from first principles have been made routinely possible for current drive prediction and direct comparison with experimental data (synthetic diagnostics)

- Bounce-averaging put limits in the range of validity in the 3-D Fokker-Planck code application: a 4-D code is a challenging physics and numerical issue.

- A lot of the experimental phenomenology is captured by ray tracing coupled with 3-D linearized, bounce-averaged relativistic Fokker-Planck solver.

- The fluctuations of the electron density may strongly modify the picture obtained with quiescent plasmas (→ convergence towards gyro-kinetic calculations)

- Consistency between of self-generated and external sources of current requires theoretical development (on going work + numerical developments → LUKE 2): wave-induced transport, bootstrap/rf wave synergy in steep gradient zones, ion physics, …